Report of Investigations No. 146

Facies Architecture and Production Characteristics of Strandplain Reservoirs in the Frio Formation, Texas

by
Noel Tyler and
William A. Ambrose

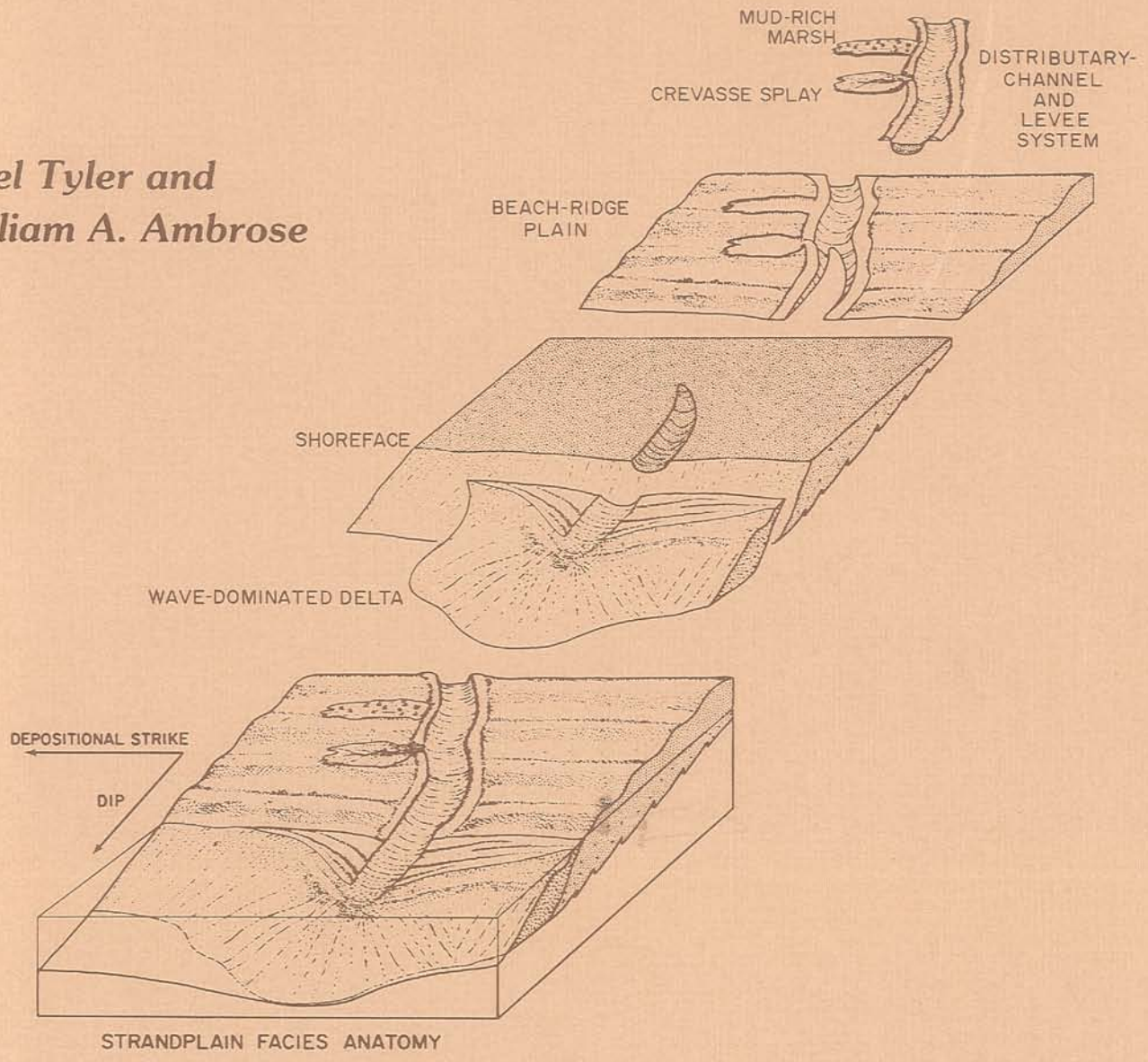

STRANDPLAIN FACIES ANATOMY

1985

Bureau of Economic Geology
W. L. Fisher, Director
The University of Texas at Austin
Austin, Texas 78713

Report of Investigations No. 146

Facies Architecture and Production Characteristics of Strandplain Reservoirs in the Frio Formation, Texas

by
Noel Tyler and
William A. Ambrose

1985

Bureau of Economic Geology
W. L. Fisher, Director
The University of Texas at Austin
Austin, Texas 78713

CONTENTS

Figures

Table

ABSTRACT

Many modern shore zones comprise a continuum of depositional environments that encompass both strandplain and barrier-island systems. Strandplains are further subdivided into two classes: sand-rich beach-ridge plains and mud-rich chenier plains. Tertiary shore-zone systems of the Texas Gulf Coast Basin contain a significant proportion of the Texas oil resource in clastic reservoirs. These reservoirs display better-than-average oil recovery efficiencies. This report describes the production attributes of three Frio strandplain reservoirs—the Cayce, the Cornelius, and the Carlson—in the North Markham–North Bay City field, Matagorda County, Texas.

Hydrocarbons in the North Markham–North Bay City field were trapped in a simple rollover anticline. Oil is produced from stacked strandplain sandstones in this multiple-reservoir field. Composite sandstones of beach-ridge plain/distributary/delta-front origin constitute the Cayce oil reservoir. Internal heterogeneity results in considerable fluid-flow anisotropy, as displayed by sequential water-cut maps and oil production maps. Water influx in the strandplain deposits follows broad fronts, whereas water invasion in channel deposits is more restricted and erratic. The Cornelius reservoir was deposited in a system intermediate between sand-rich beach plains and mud-rich chenier plains. Sandy beach ridges, separated by muddy swales, compose the productive framework of this class of strandplain reservoir and furthermore act as conduits for early water influx. Sandstones, possibly of washover origin, in the intervening swales produce oil but are more rapidly drained than are beach-ridge sandstones. The Carlson reservoir produces from transgressed strandplain deposits. Oil is contained in upward-fining transgressive sandstones that rest on thicker but oil-barren progradational facies. Facies analysis indicates that the Carlson had a complex and episodic depositional history, yet water-influx maps and oil production maps suggest isotropic fluid behavior. Modern sand-rich transgressive shore-zone deposits are characteristically sheetlike, as is the transgressive component of the Carlson reservoir. This distinctive morphology appears to have fostered reservoir productivity.

Oil recovery from the North Markham–North Bay City reservoirs follows a predictable trend. Recovery efficiency is highest from the transgressive sheet sands of the Carlson, which is the shallowest of the major oil reservoirs; intermediate from the composite Cayce; and lowest from the depositionally complex and mud-rich Cornelius, which overlies the Cayce. Reservoir efficiency of the strandplain sandstones in the North Markham–North Bay City field exceeds that of barrier and back-barrier deposits productive elsewhere in the Frio Formation of the central Texas Gulf Coast.

Keywords: *Texas Gulf Coast, Matagorda County, Frio Formation, North Markham–North Bay City oil field, strandplain reservoirs, reservoir architecture, oil production*

INTRODUCTION

Strandplain and barrier-island deposits compose an important class of oil reservoir in Texas. They contain approximately 12 percent of Texas' in-place oil resource in clastic rocks and display an above-average recovery of 50 percent (Tyler and others, 1984). Using the North Markham–North Bay City field area as an example, this report documents the relation between facies architecture and production characteristics of three Tertiary strandplain reservoirs (Cayce, Cornelius, and Carlson) in the Frio Formation, Texas Gulf Coast Basin. A companion report (Galloway and Cheng, 1985) describes results of a similar study of back-barrier reservoirs in the West Ranch field, Jackson County, Texas.

Strandplain Depositional Systems

Strandplains are marine-process-dominated depositional features welded onto coastal mainlands (fig. 1). In contrast, barrier islands are separated from the adjacent coastal plains by extensive lagoons or bays. Strandplains are classed into two broad groups: sand-rich beach-ridge plains and mud-rich chenier plains. Modern examples of beach-ridge plains are the Nayarit (Curray and others, 1969) and the Tabasco (Psuty, 1967) coastal plains of Mexico. The best-known chenier plains are those of southwestern Louisiana (Fisk, 1955; Beall, 1968; Otvos and Price, 1979; and others) and the Guianas of South America (Brower, 1953; Wells and Coleman, 1981a, b).

Beach-ridge plains and chenier plains are dominantly progradational features, shaped by the relations among sediment texture and rate of supply, coastal physiography (including slope), and wave and tidal energy. An abundant supply of mud is required for the development of chenier plains (Otvos and Price, 1979). The Mississippi River provides sediment for the west Louisiana cheniers, and the Amazon and Orinoco Rivers supply clay and silt to the coastal mud plains of the Guianas. Chenier plains, beach-ridge plains, and barrier islands can occur as a continuum, as exemplified by the microtidal regressive coastline of the Gulf Coastal Plain west of the Mississippi River. From the spatial arrangement of mud- and sand-rich strandplains and barrier islands, their vertical superposition in the stratigraphic column can be predicted. Indeed, this is true for the upper Frio in the North Markham–North Bay City field area.

The relative proportion of fine-grained to coarse-grained clastics and the facies architecture of beach-ridge plains and chenier plains differ greatly (figs. 2 and 3). Component facies of beach-ridge plains are (1) a sandy beach-ridge complex, which is the most widespread of the strandplain facies (fig. 2), (2) crosscutting fluvial-deltaic complexes, and (3) a sandy shoreface. In chenier plains (1) tidal, or storm-influenced, interridge mud flats are the most widespread depositional environment (fig. 3); (2) shelly sand ridges (cheniers) are widely dispersed on the mud flats; (3) fluvio-estuarine complexes transect the plain; and (4) a sandy to silty shoreface lies seaward of the chenier plain.

Beach-Ridge Plains

The *beach-ridge complex* is a strike-elongate, commonly curvilinear mass of prograded beach ridges. Individual beach ridges are subparallel and compose a series of subcomplexes bounded by small-scale erosional unconformities (fig. 2). Well-sorted shoreface, beach, and dune sands compose the complex. Seaward-oriented accretionary foresets separate beach ridges (fig. 2), but internal stratification is only crudely preserved, having been largely destroyed by burrowing.

Crosscutting *fluvial-deltaic complexes* consist of dip-elongate, upward-fining channel sandstones that terminate in strike-parallel, upward-coarsening to massive, wave-dominated delta deposits. Dominant channels erode through the beach ridges and transect their strike-parallel trend, whereas lesser channels are commonly diverted by the beach ridges and flow parallel to strike (fig. 2A). Abandonment of the lesser channels commonly results in a mud plug. Channel sandstones display

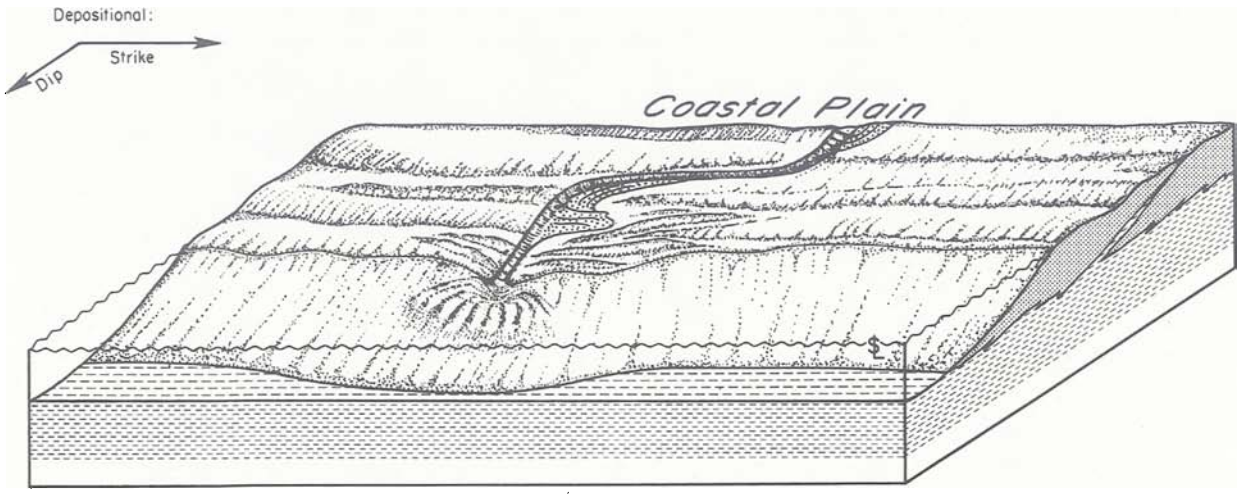

A. Sand-Rich Strandplain (Beach-Ridge Plain)

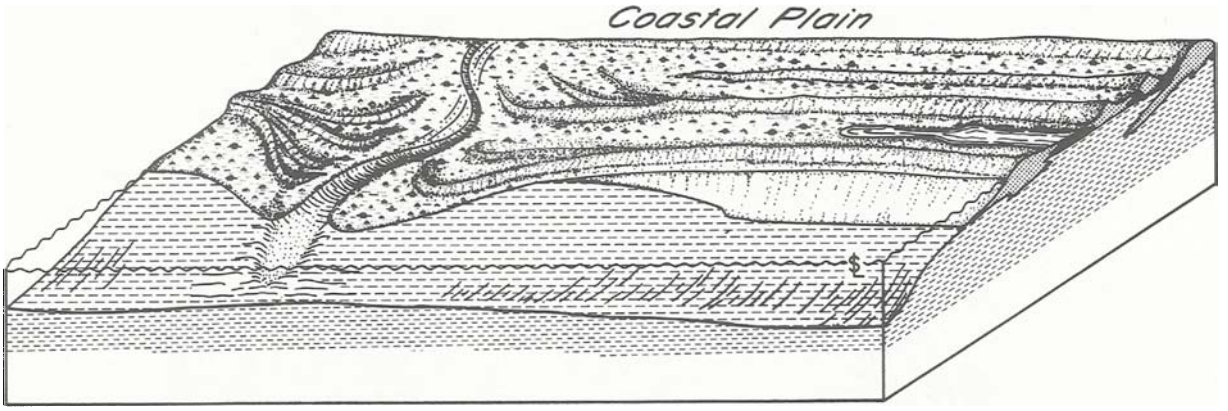

B. Mud-Rich Strandplain (Chenier Plain)

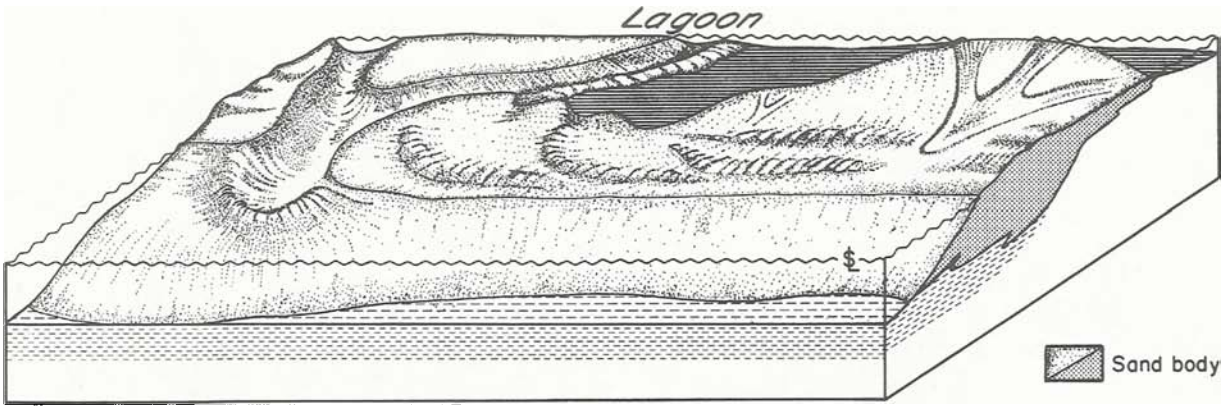

C. Barrier Island

QA-2274

Figure 1. Schematic models illustrating the principal environments of deposition in (A) beach-ridge plain, (B) chenier plain, and (C) barrier-island systems (from Galloway and Cheng, 1985).

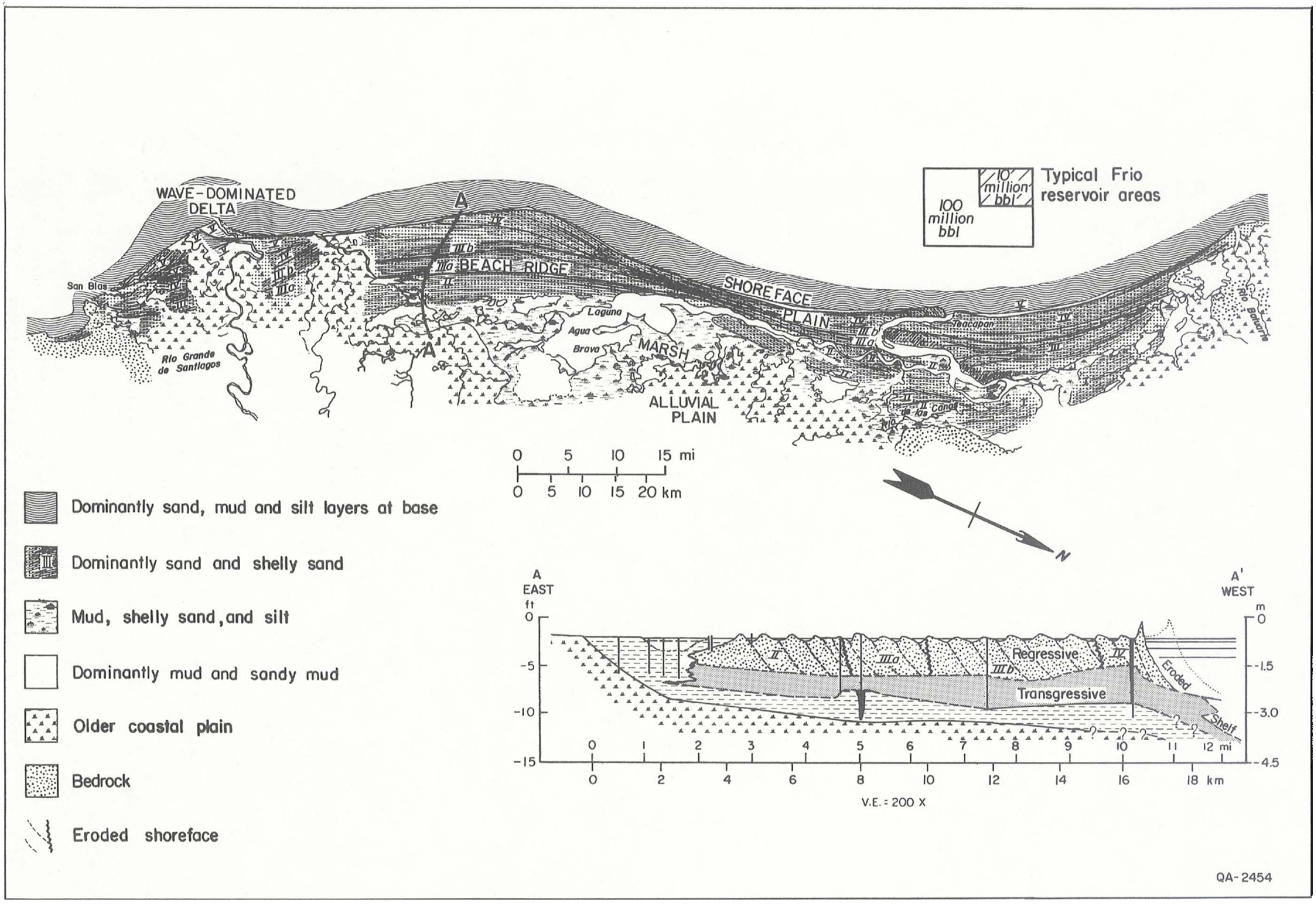

Figure 2. Physiography of a modern beach-ridge strandplain, Nayarit coastal plain, Mexico, and a cross section illustrating the tabularity of prograding beach-ridge deposits (from Curray and others, 1969).

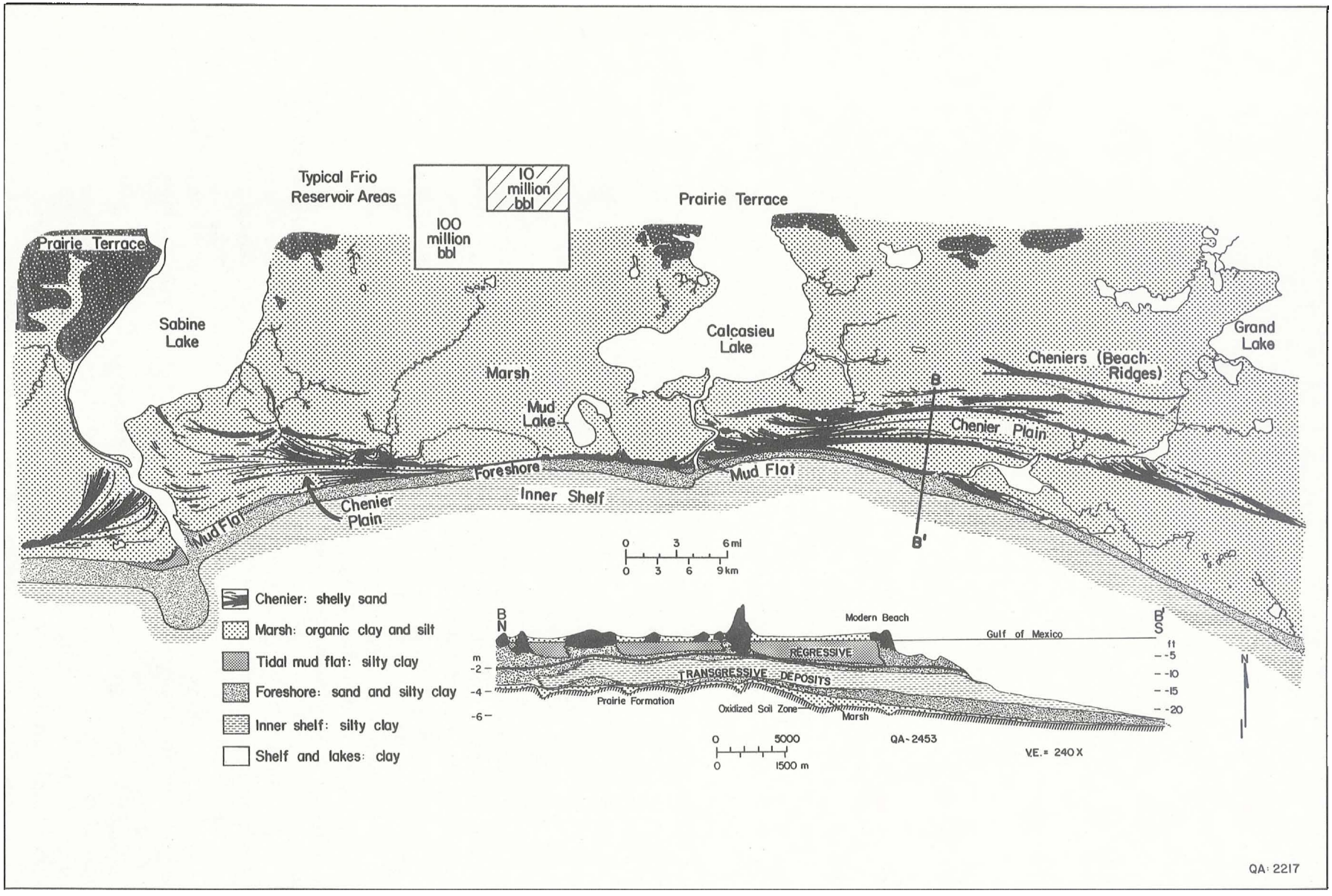

Figure 3. Physiography of a modern chenier plain, western Louisiana, and a cross section illustrating the shallow-based and irregular distribution of chenier plain beach ridges (from Gould and McFarlan, 1959).

erosive contacts and are weakly stratified at the base; hence, stratification increases vertically. In contrast, the textural maturity of the delta sands increases vertically, and internal stratification is moderate.

The *shoreface* lies seaward of and parallel to the beach plain. The shoreface contains the finest of the coarse clastics and is transitional in position and in grain size between coarser beach and dune sands and lower shoreface to shelf muds. Grain size increases vertically. Stratification, which is most strongly developed near the base of the shoreface, is rarely preserved because of intense bioturbation.

Chenier Plains

Tidally influenced *mud flats* compose the bulk of the sediment of chenier plains. Mud flats not only separate sand ridges but also may be the floor upon which certain cheniers are built (fig. 3). They are very fine grained, exhibit an upward-fining textural trend, and originate in part from sedimentation in protected swales behind upper-shoreface breaker bars. Mud flats are therefore highly stratified. During progradation, abandoned mud flats become colonized by marsh or mangrove vegetation.

Cheniers are strike-elongate, narrow, shelly sand bodies that compose the ridges separating mud flats on chenier plains. They exhibit bifurcating morphologies and tend to fan out as they approach estuaries (fig. 3). Two processes account for their origin. During periods of low sediment supply, waves winnow the intertidal mud flats and concentrate the coarser clastic and shelly detritus into beach ridges, forming cheniers that rest on shoreface clays and exhibit upward-coarsening textural trends. Alternatively, storm-washover processes may build cheniers on marsh deposits. The resulting sand ridges are abruptly based and upward fining.

Fluvioestuarine complexes may transect the chenier plain. These minor rivers contribute little or no sediment to the chenier plains because the estuaries into which they flow act as sediment sinks. The streams are often diverted by the cheniers and flow parallel to the coast. Texturally, fluvioestuarine deposits are upward fining or are mud-rich and massive; they are erosively based and dip-elongate.

Chenier plain shoreface deposits coarsen upward from shelf muds into the fine sand of the breaker-bar zone of the inner shoreface. Aggradation of the breaker-bar system into a protective shoaling ridge allows deposition of suspended sediment in the swale behind the ridge and formation of broad intertidal mud flats (Beall, 1968). Shoreface deposits are strike-elongate and highly stratified.

Oil-Bearing Strandplain Systems of the Texas Gulf Coast Basin

Three barrier/strandplain systems that produce oil and gas have been recognized along the Texas Gulf Coast (Galloway and others, 1983). (1) South Texas fields in the Eocene Jackson-Yegua barrier/strandplain trend produce from the landward margins of thin barrier/strandplain sandstones; oil is trapped primarily by updip stratigraphic pinch-outs. The two shore-zone systems in the Oligocene Frio Formation flank the Houston delta system (Galloway and others, 1982). (2) The Buna barrier/strandplain system, which lies to the east of the Houston delta system, contains only three major reservoirs (those with cumulative productions greater than 10 million barrels). Production takes place from the seaward margins of thick sandstones warped over salt domes and from rollover anticlines and faulted anticlines. (3) The Greta-Carancahua barrier/strandplain system of the Frio Formation was deposited in a coastal bight between two Tertiary deltaic depocenters (fig. 4). This oil play contains 46 major reservoirs—the most of any play in the Texas Gulf Coast Basin (Galloway and others, 1983). The main producing sands lie landward and seaward of the shore-zone depositional axis, where back-barrier and fore-barrier deposits are sealed by lagoon and shelf mudstones, respectively. Simple and faulted anticlines are the dominant traps, formed by warping over shale-cored diapirs and growth-fault rollover anticlines (Galloway and others, 1982). North Markham–North Bay City is one of the fields in this play and is located downdip of the shore-zone depositional axis near the Houston delta system (fig. 4).

Major oil reservoirs in barrier/strandplain systems of the Texas Gulf Coast Basin contained more than 5.5 billion barrels of original oil in place. Reservoirs in these systems, particularly in the shore-zone core and shoreface settings, are typified

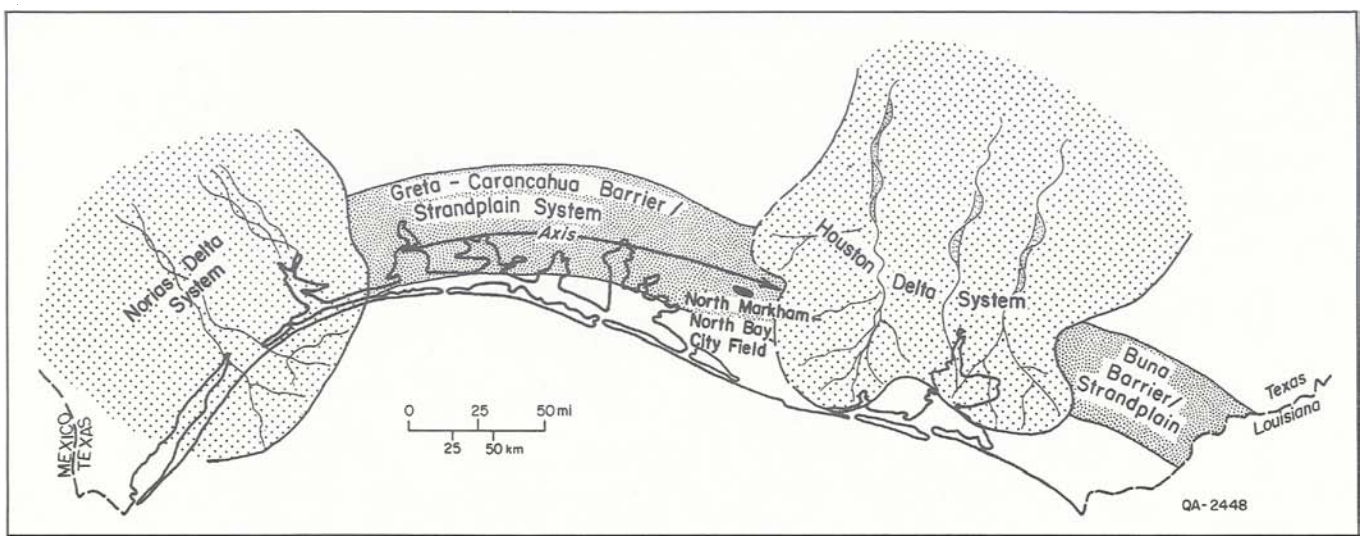

Figure 4. Frio depositional systems (from Galloway and others, 1982) and location of the North Markham–North Bay City field.

by high porosity and permeability values (31 percent and 1,300 md, respectively) and by water- or combination-drive mechanisms. Consequently, recovery from these laterally continuous, well-sorted sandstones is high, averaging 53 percent. This is significantly higher than the average recovery of 41 percent from clastic reservoirs in Texas (Tyler and others, 1984). Back-barrier reservoirs, such as along the Jackson-Yegua trend, are commonly lenticular and are driven by solution gas. Recoveries from back-barrier reservoirs are only moderate, averaging 38 percent.

NORTH MARKHAM–NORTH BAY CITY FIELD

The North Markham–North Bay City field produces oil and gas from multiple stacked barrier and strandplain sandstones of the upper Frio Formation. The field lies seaward of the strike-elongate axis of upper Frio shore-zone sediments (fig. 4), which are composed of thick sandstones that characteristically exhibit a blocky spontaneous potential (SP) response (fig. 5; wells 124,124A). Interbedded mudstone content is lowest along the shore-zone axis and increases away from this zone of thickened sandstones landward and seaward. Three sedimentation cycles are contained in the depositional axis, which is centered in the Markham salt-withdrawal basin. Cycle 1, the lower cycle (fig. 5), records prograding-barrier sedimentation. Landward of the barrier axis, thin sandstones rapidly feather out into thick lagoonal mudstones. Cycle 2 was characterized by aggradation coupled with coastal onlap. In contrast to sandstones of cycle 1, sandstones landward of the depositional axis are thin, but persistent, and are interbedded with equally thin mudstones. These sediments were deposited on a marshy coastal plain that was criss-crossed by meandering streams preserved as thicker, upward-fining lenticular sandstones. On the basis of the absence of thick lagoonal mudstones landward of the shore-zone axis, cycle 2 represents a phase of strandplain sedimentation. In cycle 3, barrier-formation conditions returned with the deposition of the Greta barrier/ lagoon system. Back-barrier deposits of cycle 3 consist of lagoonal mudstones and thin sandstones.

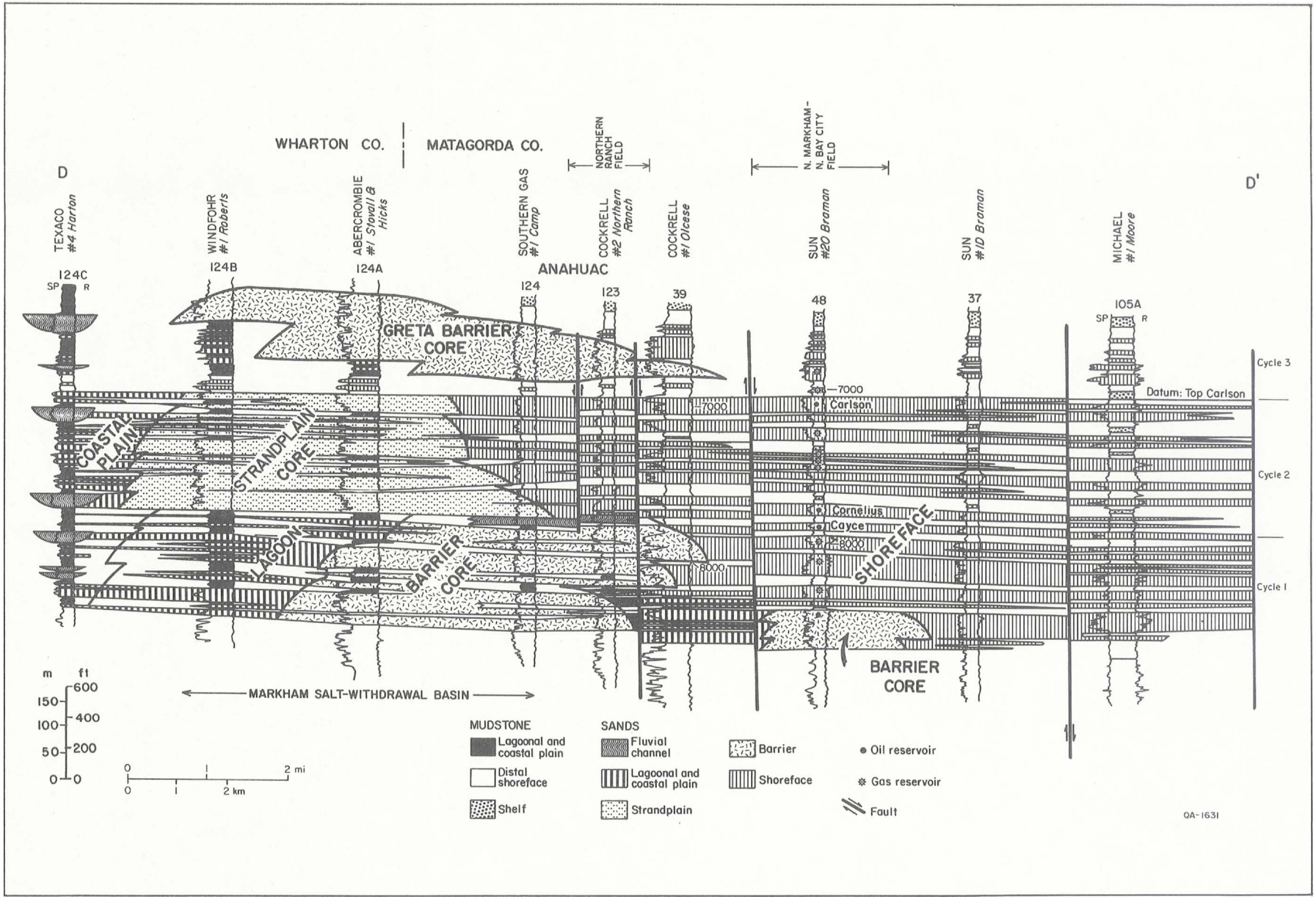

Figure 5. Upper Frio stratigraphic dip cross section. The field area lies downdip of the Greta-Carancahua barrier/strandplain core and produces from extensive barrier and strandplain sandstones. Location of section is shown in figure 6.

In contrast to the thin and laterally discontinuous sandstones landward of the depositional axis, sandstones seaward of the axis exhibit remarkable continuity (commonly more than 10 mi, 16 km; fig. 5), regardless of their origin. The three main oil reservoirs of the field, the Carlson, Cornelius, and Cayce, produce from tabular strandplain sandstones of cycle 2 (fig. 5). The Carlson, which is the uppermost oil reservoir, lies directly below transgressive shoreface and shelf mudstones that seal the reservoir. The Carlson is a composite progradational transgressed sandstone that exhibits a complicated facies architecture. The Cornelius reservoir produces from a prograded mud-rich strandplain deposit, and the Cayce from composite strandplain/distributary/wave-dominated delta sandstones. Reservoir heterogeneity is greatest in the Cayce and Cornelius reservoirs.

Contemporaneous growth faulting was the dominant structural process during deposition of the Greta-Carancahua barrier/strandplain system. Faulting produced shale-cored, strike-elongate rollover anticlines, such as the double-crested anticlinal trap in the North Markham–North Bay City field (fig. 6), downdip of the fault planes. The relative structural elevations of the twin domal crests of the anticline vary with depth (fig. 7). Structural closure of the west dome is greatest in the shallower sandstones so that in these reservoirs (including the Carlson), oil and gas are confined to the western half (North Markham) of the field. Hydrocarbons occur in both domes at intermediate depths (including the Cornelius and Cayce reservoirs); however, the deep gas reservoirs produce mainly from the east dome.

Oil Production from the North Markham–North Bay City Field

In the early years of oil production, the North Markham and North Bay City field areas were operated separately. The west half of the field (North Markham) was discovered in 1938 with the completion of the Ohio Cornelius No. 1 well in the Cornelius reservoir. Production from the east dome was established with the completion of the Ohio McDonald Account No. 1 well in the Cayce reservoir in 1942. For the following 10 years, the two domes were produced as discrete fields under two sets of field rules.

Recognition of continuous hydrocarbon zones and of pressure continuity between the two domes in reservoirs of intermediate depths led to a joint engineering study by the individual operators. In 1952 the two fields were consolidated and subsequently unitized to form the North Markham–North Bay City field. By 1969 the Railroad Commission of Texas had recognized 20 separate hydrocarbon reservoirs in the field; 9 are principally oil reservoirs and the remaining 11 are gas reservoirs. Cumulative oil production by the end of 1982 was 44.4 million barrels, and total gas production, including casinghead gas for 1982, was 1.1 Bcf (Railroad Commission of Texas, 1983). Production from the reservoirs considered in this study amounted to 40.3 million barrels (Carlson, 13.1 million barrels; Cornelius, 17.4 million barrels; and Cayce, 9.8 million barrels) by the end of 1982.

Geologic, engineering, and fluid characteristics for the three reservoirs are summarized in table 1. Reservoir production energy is supplied by water drive supplemented by gas-cap expansion. Average porosities range from 24 to 31 percent, and average permeabilities from 750 to 3,300 md. The mud-rich Cornelius reservoir displays consistently lower porosity and permeability values and higher residual oil saturations than the other two reservoirs. All three reservoirs produce moderately high gravity oil (35° to 36° API) with low original gas-to-oil ratios (600 standard ft^3/stocktank barrel) and have undergone pressure maintenance by gas injection. Ultimate recovery of oil ranges from 61 percent from the Cornelius reservoir to 70 percent from the Carlson reservoir.

Facies Influence on Reservoir Continuity

The influence of physical and textural variations on clastic-reservoir performance is attracting increasing attention (Polasek and Hutchinson, 1967; Alpay, 1972; Hartman and Paynter, 1979; and others). In the past, engineering practice assumed reservoirs to be either homogeneous and isotropic or weakly anisotropic (Alpay, 1972). However, the hard lessons learned from several decades of enhanced recovery have confirmed that a thorough

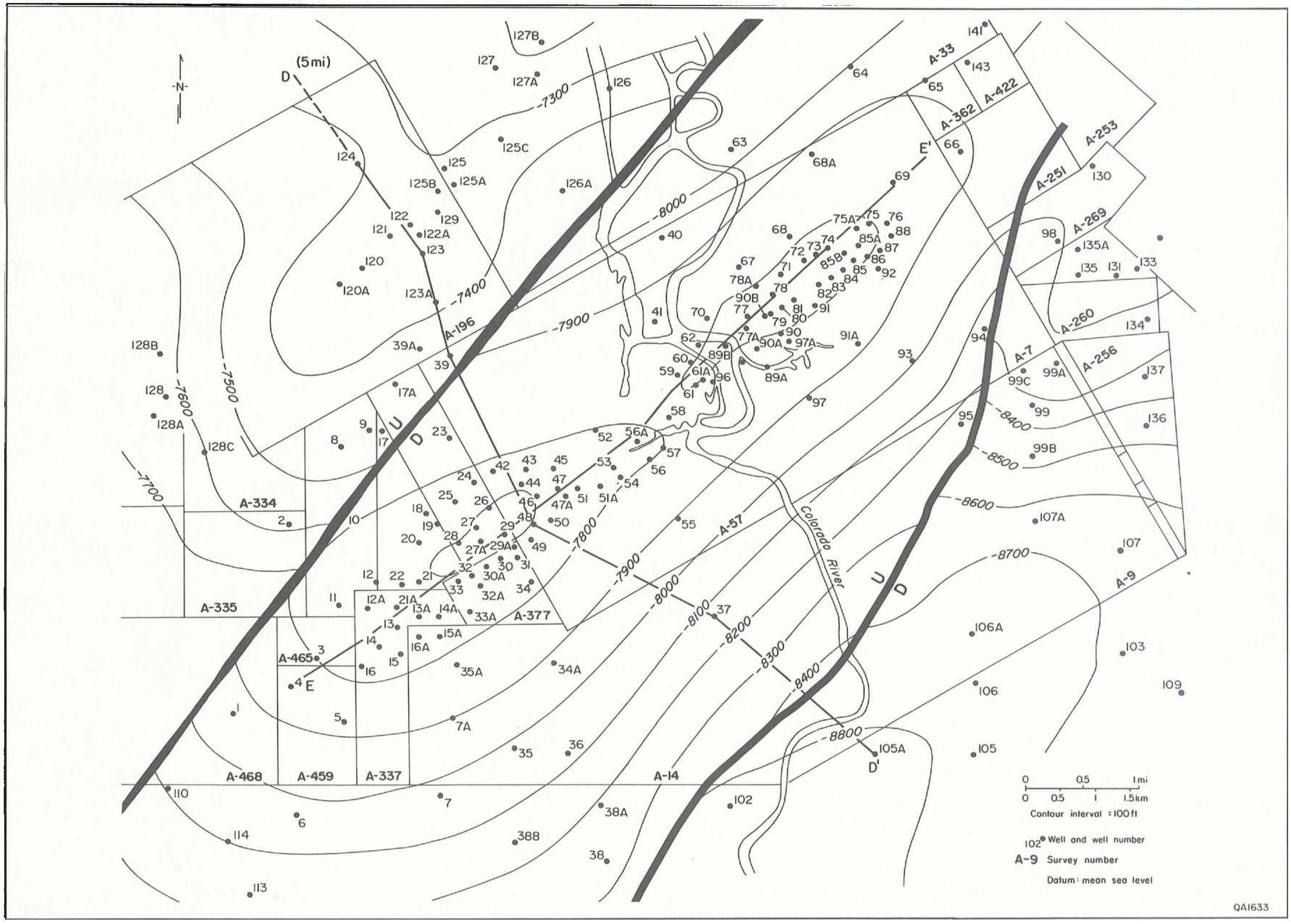

Figure 6. Structure map of the North Markham–North Bay City field contoured on top of the Cayce sandstone. Sections D and E shown in figures 5 and 7, respectively.

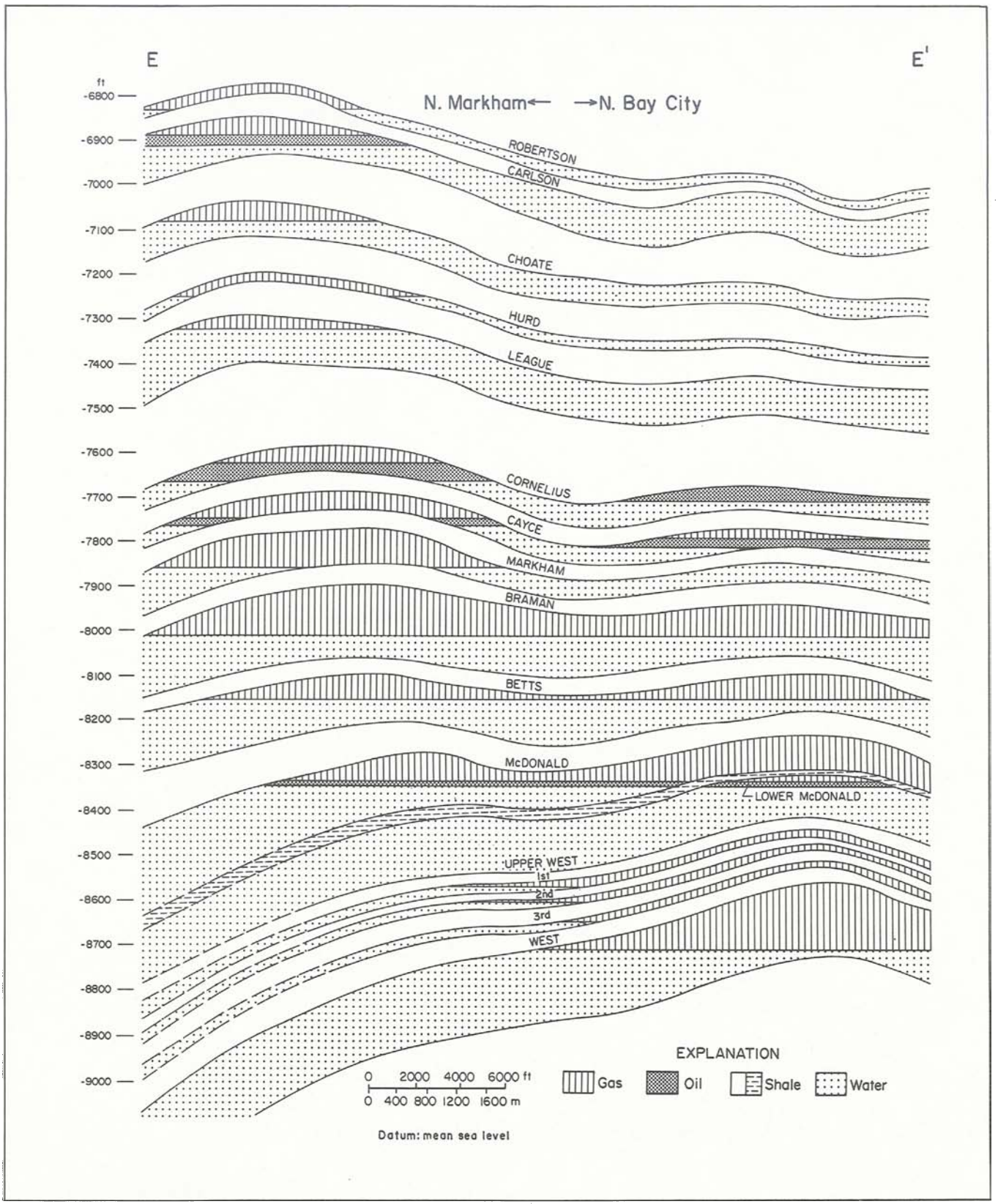

Figure 7. Generalized west-east section across the North Markham–North Bay City field. Principal oil reservoirs are the Cayce, Cornelius, and Carlson. Section shown in figure 6. Modified from Marathon Oil Co., Railroad Commission of Texas Docket No. 3-23116, exhibit 2.

Table 1. Geologic, fluid property, engineering, and production characteristics of the principal oil reservoirs of the North Markham–North Bay City field.*

	Reservoir		
	Carlson	*Cornelius*	*East Cayce*
Discovery date	1938	1938	1942
Lithology	SS	SS	SS
Trap	Rollover anticline	Rollover anticline	Rollover anticline
Drive	Water drive and gas-cap expansion	Water drive and gas-cap expansion	Water drive and gas-cap expansion
Depth (ft/m)	7,000/2,134	7,700/2,347	7,800/2,377
Oil column (ft/m)	25/8	40/12	20/6
Porosity (%)	31	26	28.5
Permeability (average md)	3,333	293	1,737
Permeability (log range)	2-3	2-3	2-3
Initial water saturation (%)	26	28	30
Residual oil saturation (%)	28‡	No data	No data
API gravity (°)	36	36	35
Initial gas-to-oil ratio (scf/STB)	600	640	628
Initial pressure (Psig)	3,190	3,572	3,623
Temperature (°F/°C)	182/83	193/89	196/91
Pressure maintenance	gas injection	gas injection	gas injection
Unitization date	52	52	52
Well spacing (acres)	40	40	40
Original oil in place (million barrels)	20	36	15.7
Cumulative production (million barrels)	13.1	17.4	9.8
Ultimate recovery (million barrels)	14.0	22.0	10.4
Recovery efficiency (%)	70	61	66

*Data from hearing files at the Railroad Commission of Texas.
‡This value appears to be anomalously high when compared to other Frio reservoirs that display residual oil saturation values of 10 to 20 percent; 15 percent would probably be a better approximation.

understanding of the internal architecture of reservoir facies is needed to develop realistic models for predicting and evaluating reservoir behavior. Variations in the internal properties of depositional units (grain-size distribution, pore-space distribution, permeability, porosity stratification, frequency and position of shale breaks) are responses to changes in depositional

processes. Amalgamation and superposition of depositional facies because of these variations result in composite sandstone bodies and ultimately in heterogeneous reservoirs. Studies of modern environments (Pryor, 1973) and of oil field production characteristics (such as that of Hartman and Paynter, 1979) indicate that physical and textural characteristics of sand facies and abrupt changes in these characteristics at facies boundaries clearly influence rates and paths of fluid flow.

Three levels of reservoir heterogeneity affect or control fluid flow in sandstones (Alpay, 1972). Megascopic heterogeneity is the regional or fieldwide (interreservoir) variation in sandstone character; macroscopic heterogeneity is the well-to-well (intrareservoir) variation, and microscopic heterogeneity is the pore-to-pore variation. Areal and vertical textural contrasts (macroscopic heterogeneity) and megascopic heterogeneity, such as facies distribution and geometry, are the principal concerns of this study.

CAYCE RESERVOIR: A COMPOSITE PROGRADATIONAL STRANDPLAIN/ FLUVIODELTAIC COMPLEX

Depositional Environment

Thickness Trends and Sandstone Distribution

An updip growth fault strongly influenced thickness trends in the Cayce sandstone (figs. 8 and 9). This reservoir is thickest adjacent to the fault and thins over the anticlinal crest, suggesting that the anticline was bathymetrically positive during deposition of the Cayce. The interval expands downdip of the anticline and then thins toward the south. The downdip fault, which has a displacement of 200 to 400 ft (60 to 120 m), was not active during deposition of the Cayce sandstone and did not influence its thickness.

Net- and percent-sandstone contents decrease as the Cayce interval thins over the anticline (figs. 8 and 9). Thicker accumulations of sandstone were deposited on the flanks of the anticline, the major zone of sandstone deposition being seaward and east of the anticline. A second area of sandstone accumulation lies on the updip side of the growth fault.

Areal Distribution of Component Facies

The SP log character of the Cayce sandstone varies greatly throughout the field and surrounding area. In the western half of the fault block, log patterns are commonly serrate; thin sandstones define upward-coarsening cycles (fig. 9). Upward-fining and blocky patterns, locally present in the western half of the field, dominate the eastern half. Recognition of progradational and aggradational facies, as well as areas in which these two primary building blocks are mixed in varying proportions, from SP profiles (fig. 9) facilitated mapping of the architecture of component facies (fig. 10) of this composite sandstone body.

Progradational, aggradational, and mixed facies are, in turn, subdivided more specifically, as illustrated in the explanation in figure 10. Progradational and blocky SP facies are the framework of the Cayce sandstone, which is characterized over much of the area by variations of a blocky SP response; upward-coarsening log patterns are concentrated basinward. Transecting the suite of mixed and progradational facies is a north-south-oriented aggradational system consisting of simple and serrate upward-fining sandstones. Both sandstone-rich and mudstone-rich serrate log patterns are closely associated with the crosscutting system. Downdip, this aggradational facies becomes strike oriented, and the sands, although retaining their dominantly upward-fining character, become increasingly massive.

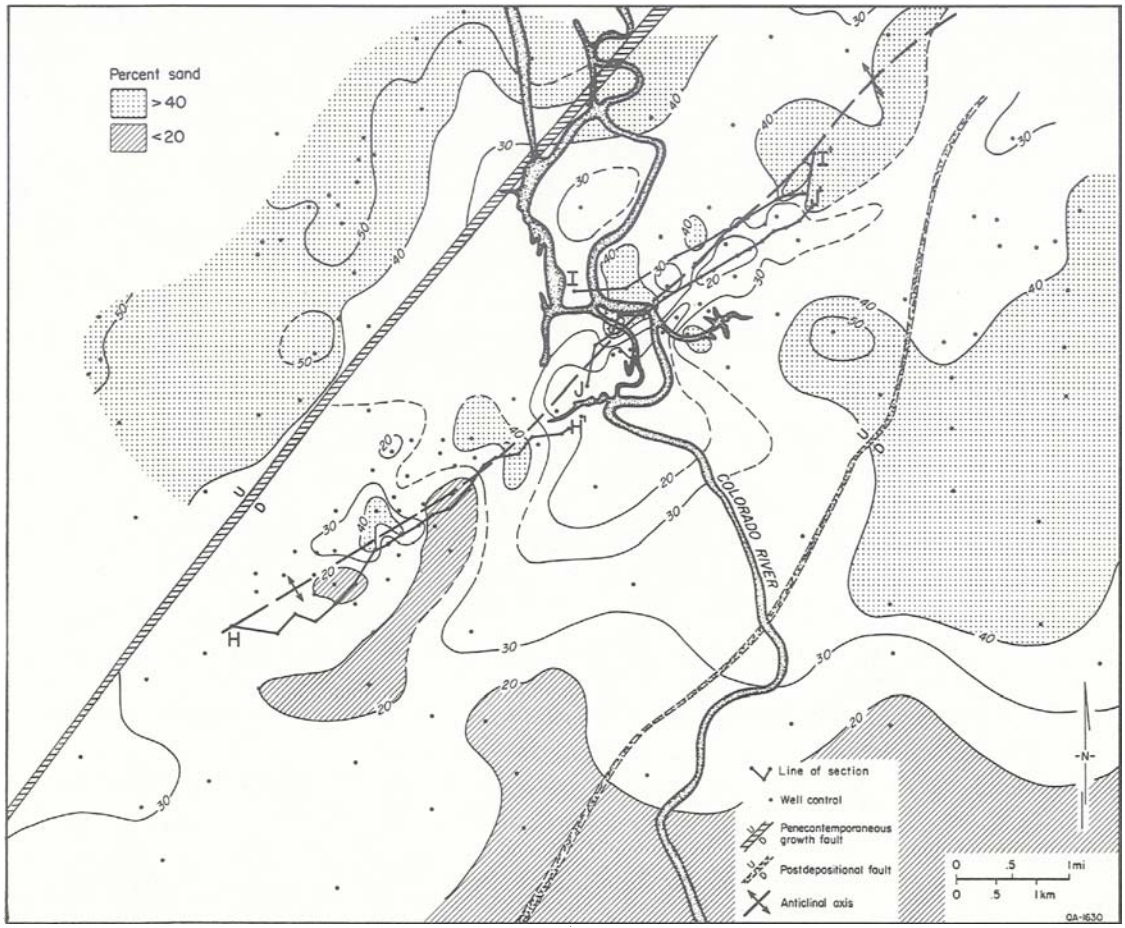

Figure 8. Percent-sandstone map, Cayce reservoir. The main area of sand accumulation downdip of the principal growth fault lies southeast of the rollover anticline. Total thickness and sandstone content of the Cayce decrease over the crest of the anticline. Section H shown in figure 14 and sections I and J in figure 13.

Interpretation of Depositional Environments

The massive sandstones that compose the bulk of the Cayce were deposited in a prograding sand-rich beach-ridge plain system. Analogous strandplain coastlines are the coastal plain of Nayarit on the Pacific Coast of Mexico (Curray and others, 1969; McCubbin, 1982) and parts of the Pleistocene Ingleside Formation along the central Texas Gulf Coast (Winker, 1979). The Cayce beach-ridge plain was transected by a river that eroded and redeposited strandplain sediments as upward-fining fluvial sandstones. From log facies data in areas of dense well control, the fluvial deposits are flanked by areally restricted sandstone-rich and sandstone-poor zones that display serrate SP responses and probably represent levee and floodplain deposits. The upper part of the river system consists of three discrete channels merging seaward into a single tract; these separate channels probably represent avulsed courses of the river. Remnant beach-ridge plain deposits separate the channels. Adjacent to the convergence zone of the channels is a local area of upward-coarsening sandstones. The restricted distribution and lobate geometry of these sandstones suggest deposition as a crevasse splay.

Downdip, the orientation of the aggradational system changes to strike-parallel (fig. 10) and the SP response becomes more blocky. Adjacent seaward deposits are typically upward-coarsening, progradational shoreface or delta-front sandstones, or both. This system of strike-parallel aggradational-to-blocky sandstones merging seaward with progra-

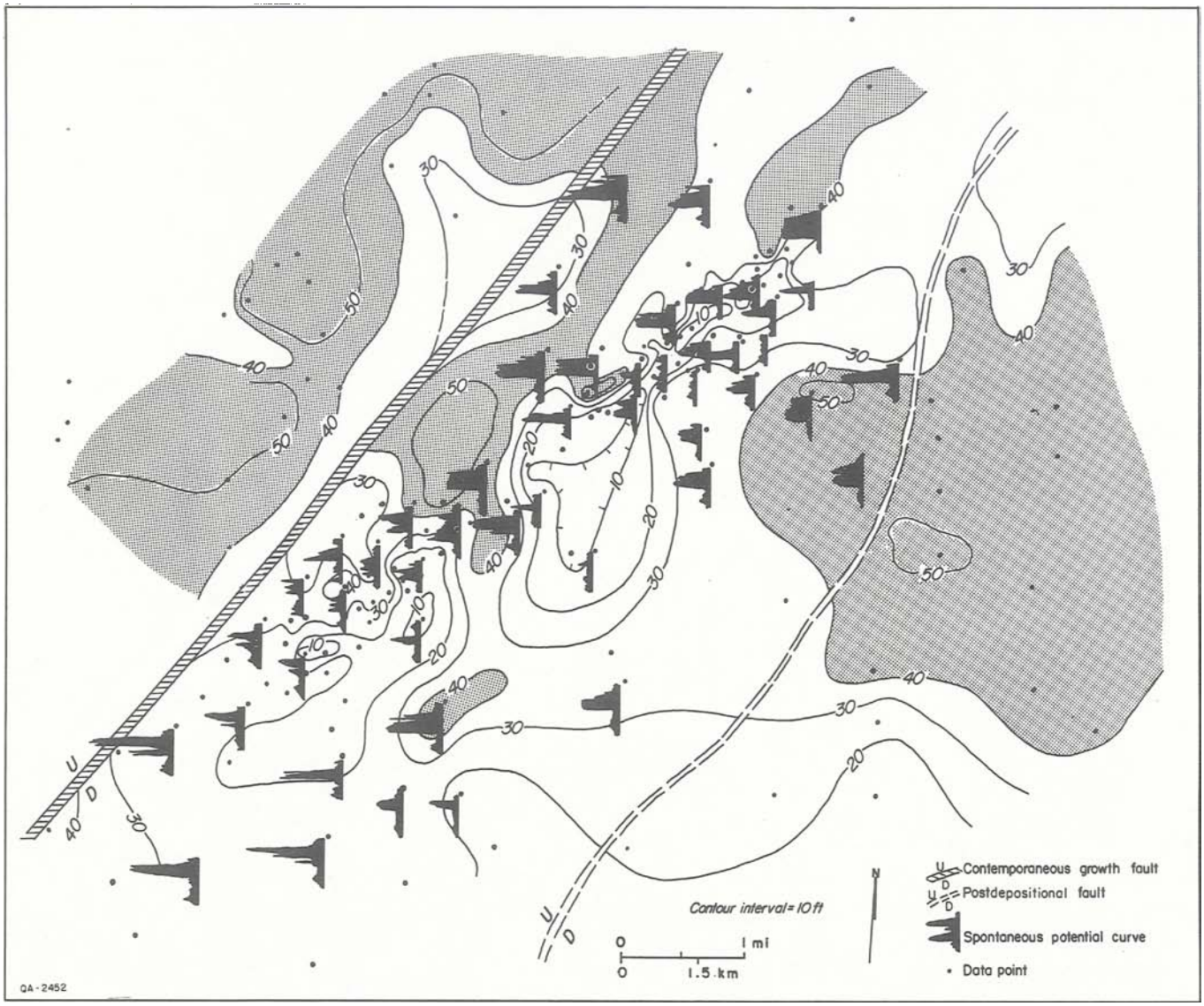

Figure 9. Log-character and net-sandstone map, Cayce reservoir.

dational sandstones is interpreted to be a wave-reworked delta. Wave-dominated deltas are integral constructional elements of beach-ridge plain shorelines (fig. 2).

Architecture and Dimensions of Component Facies

The Cayce sandstone is composed of four principal facies elements, which are, in decreasing order of areal extent, (1) a beach-ridge plain, (2) a shoreface and delta front, (3) a distributary-channel system associated with a crevasse splay and marsh that terminates in (4) a cuspate (wave-dominated) delta (fig. 11). As will be shown in this report, the production characteristics displayed by the component facies of the Cayce sandstone differ greatly.

The beach-ridge deposit is composed of a composite sandstone that is tabular in geometry and ranges from 30 to 50 ft (9 to 15 m) thick. The sandstone is laterally extensive; within the field area, it is 3 mi (5 km) long and 5 mi (8 km) wide. Modern beach-ridge plains such as the Nayarit coastal plain extend along depositional strike for

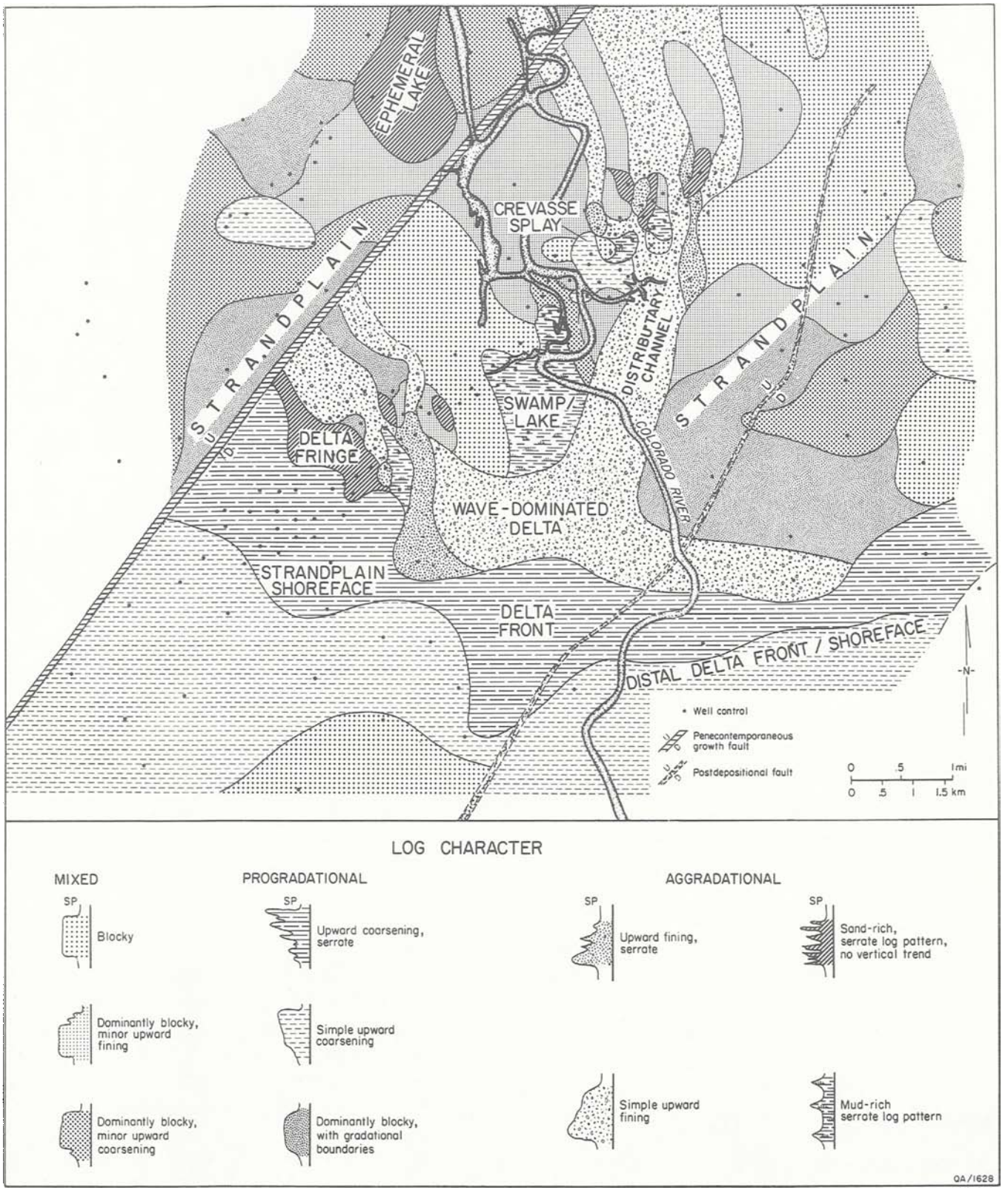

Figure 10. Facies anatomy of the Cayce sandstone, adapted from vertical SP profiles. Strandplain sandstones are crosscut by a fluvial-deltaic system that grades downdip into upward-coarsening delta-front/ strandplain-shoreface deposits.

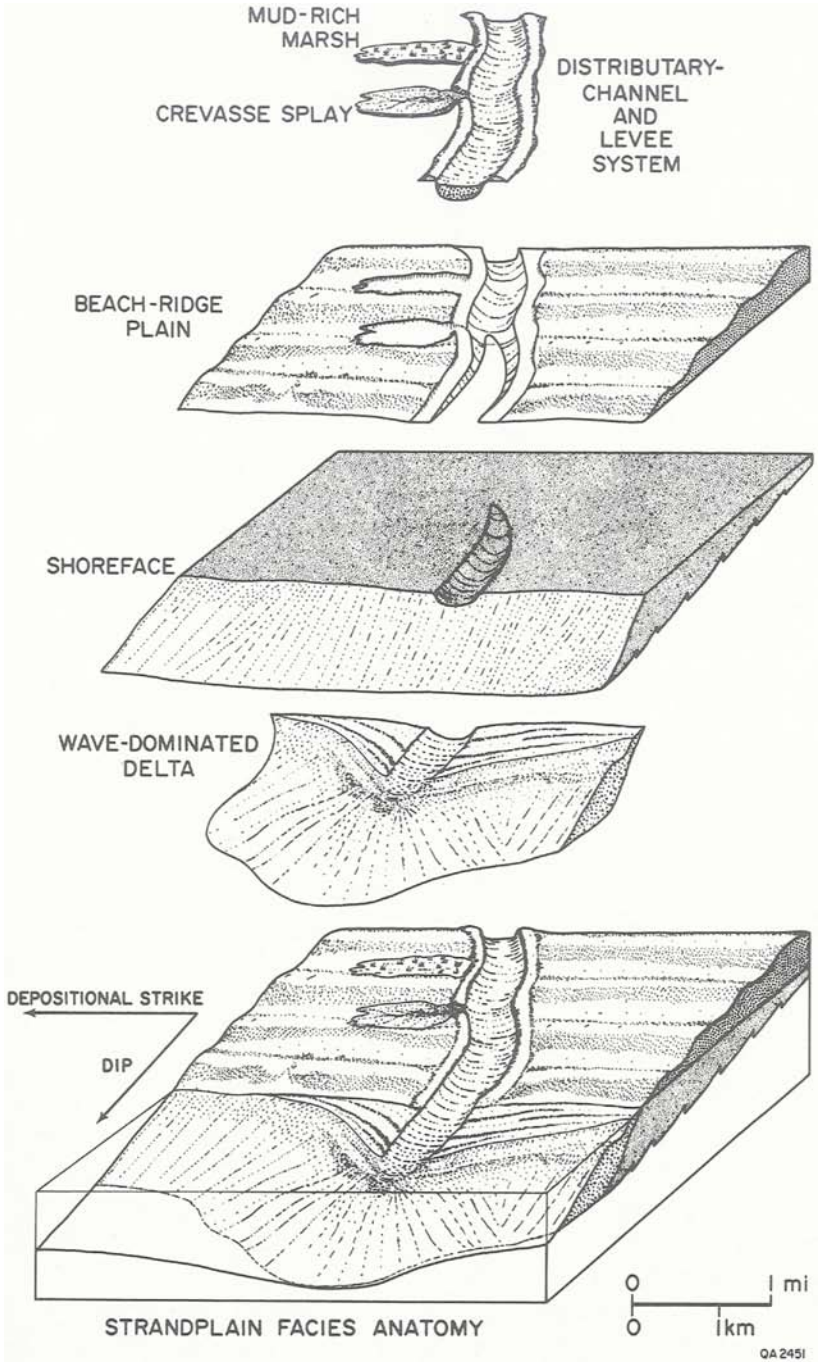

Figure 11. Exploded reservoir facies of the Cayce sandstone. The dip-elongate distributary system disrupts continuity of the tabular beach-ridge sandstone.

more than 50 mi (80 km) without interruption and display widths of between 1 and 10 mi (0.6 to 6 km). Presumably the Cayce is comparably elongate outside the field area. Composite shoreface/delta-front sandstones are equally extensive in a strike direction but are broadly lenticular in cross section.

The crosscutting fluvial system disrupts the continuity of the strandplain. The resultant deposit (0.75 mi, 1.2 km, wide and 6 mi, 10 km, long in the field area alone), which was probably deposited by several smaller rivers, is hemicylindrical, being a straight, dip-elongate body having a lenticular cross section. Adjacent to the river are smaller scale crevasse splay and levee deposits. The crevasse splay sandstone in the Cayce is a thin (0.75 mi, 1.2 km, wide), convex lenticular body aligned obliquely to paleoslope. It is sheetlike in geometry. Levee deposits that flank the channel system also exhibit a lenticular cross section but are dip elongate and discontinuous.

Sandstones deposited by the delta system display an asymmetrically cuspate geometry typical of wave-dominated deltas (fig. 2). The Cayce delta is similar in geometry and areal extent (4 mi^2, 10.4 km^2) to the modern Brazos delta of the Upper Texas Gulf Coast. Both deltas owe their cuspate geometry to rapid contemporaneous reworking of sediment by waves and currents in the Gulf Coast Basin.

Areal Stratification Trends

Maps of stratigraphic complexity show the areal variation in vertical heterogeneity in the reservoir. These maps show the number of beds intersected by the well bore in a depositional sequence. The term "beds" is used here to refer to sandstone units that are differentiated from underlying and overlying sands by shale or cemented zones. Bed boundaries are inferred from SP or resistivity deflections or both. The figures obtained this way for each well represent the stratigraphic complexity (analogous to the heterogeneity factor of Polasek and Hutchinson, 1967) in the area. The maps do not imply that actual physical boundaries exist in the reservoir where contours are drawn (Alpay, 1972).

A systematic decrease in the number of beds in the entire Cayce progradational genetic unit (from the top of the Markham to the top of the Cayce, fig. 7) takes place from updip, where there are 10 discrete strata, to downdip, where there are only 2 stacked strata. If only the main producing sandstone composed of both dip- and strike-oriented elements is considered, a more complicated pattern emerges that matches the complex facies architecture (fig. 12). The channel sandstones generally comprise few strata and therefore have low heterogeneity factors, whereas the strandplain, delta-fringe, and delta-front sandstones exhibit moderate to high heterogeneity factors. The area of low vertical heterogeneity in the middle of the field corresponds to the marsh or lake deposits that lay adjacent to the main channel.

Reservoir Continuity and Distribution of Hydrocarbons

Cross sections on which the magnitude of the resistivity deflection is contoured are most useful in documenting the lateral continuity of the component facies and their control on the areal distribution of hydrocarbons. Subtle changes in SP log facies are made more apparent by changes in the location and magnitude of the resistivity peak.

Deep-induction resistivity curves are used to distinguish hydrocarbon-bearing zones from water-bearing zones (Asquith and Gibson, 1982). The framework components and the matrix of sediments are nonconductive; thus, electrical currents are transmitted through sandstone by water contained in pore spaces. Hydrocarbons are also nonconductive; therefore, an increase in the resistivity indicates an increase in hydrocarbon saturation (Asquith and Gibson, 1982). This permits mapping of hydrocarbon distribution within component facies. The effect of different drilling muds on the resistivity response was found to be minor.

In the east Cayce reservoir continuity is greatest in beach-ridge deposits (fig. 13A). The crosscutting fluvial complex disrupts the continuity of the reservoir and imparts considerable lateral heterogeneity. Even though the beach-ridge plain and channel deposits are both sandstone-rich, the interface between these facies, possibly composed partly of fine-grained levee deposits, acts as a flow boundary. Well-completion data show that remnant

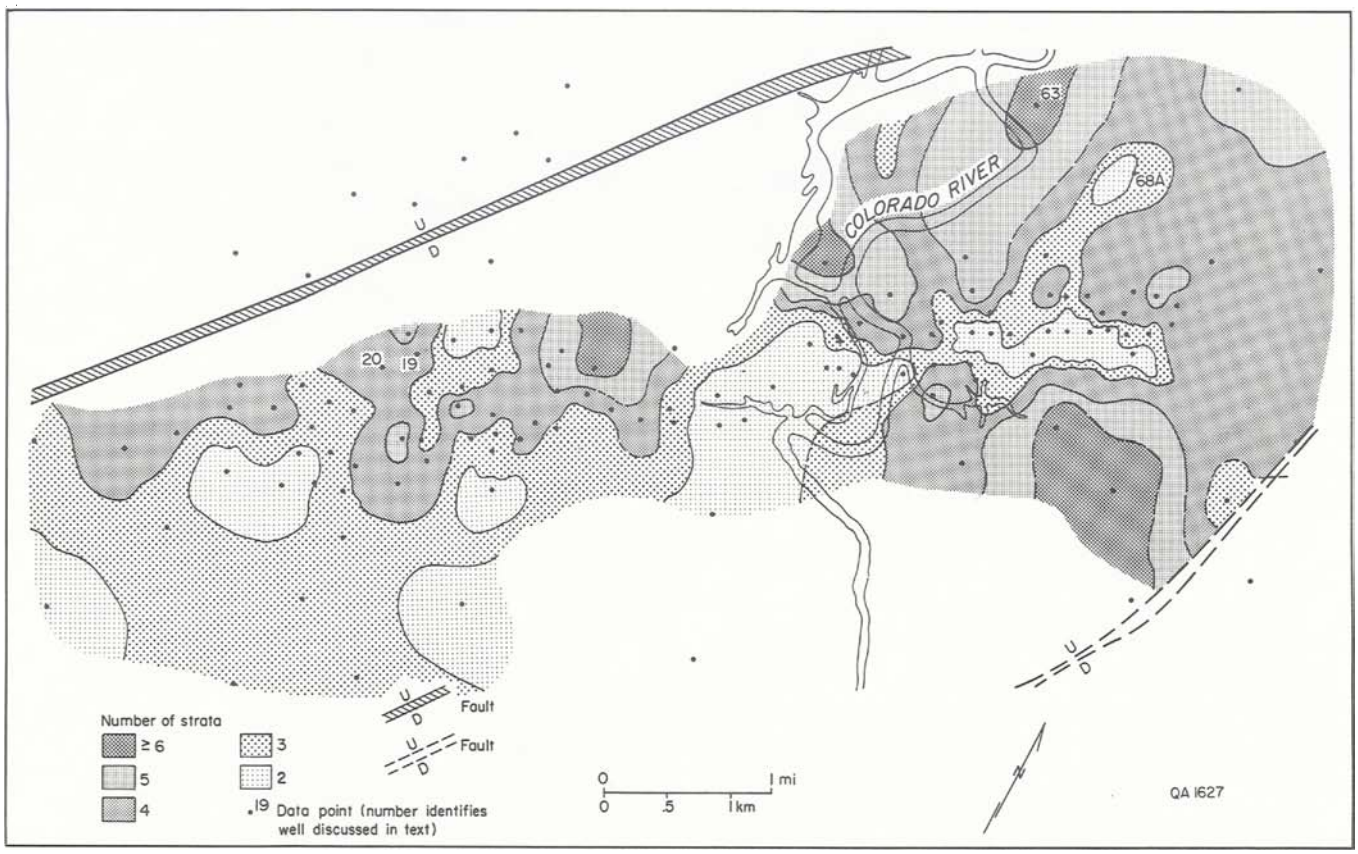

Figure 12. Stratigraphic complexity (number of strata) map of the Cayce sandstone. Resistivity or SP deflections or both are used to distinguish individual strata. In general, strandplain sandstones have more interbeds (that is, higher vertical heterogeneity) than do fluvial-channel sandstones.

strandplain deposits isolated within the channel complex exhibit lower initial production than do the adjacent channel sandstones. For example, wells 71 and 74, which were both completed in remnant beach-ridge plain deposits, initially produced an average of 182 barrels per day, whereas well 72, completed in the channel sandstone separating the two beach-ridge remnants, yielded 225 barrels per day (fig. 13B). The two facies clearly have different production characteristics. Without whole-core data, it is difficult to determine whether the differences are a result of permeability variation or of disparity in distribution of original oil in place. However, fluid flow between the two facies is clearly restricted.

The lower production from the sandstones of the remnant beach-ridge plain isolated in the fluvial complex is anomalous when compared to production from beach-ridge plain sandstones over the entire east Cayce reservoir. Average initial production from beach-ridge deposits of the east Cayce exceeds that for fluvial-channel sandstones by 50 barrels per day. (Production from beach-ridge plain sandstones averages 248 barrels per day; production from fluvial-channel sandstones averages 194 barrels per day.) Production from the associated crevasse splay sandstones is the lowest of all Cayce sandstone facies, averaging 90 barrels per day.

Continuity in west Cayce reservoir matches that in east Cayce, hydrocarbon saturation being most persistent in shoreface/delta-front deposits and least continuous in the channel sandstones (fig. 14). At the northeast contact between channel and beach-ridge plain facies (between wells 50 and 47A), a thick zone of hydrocarbon saturation in the beach-ridge plain core flanks the channel complex. Had fluids been able to move freely between facies, hydrocarbon saturations would have equilibrated. Instead, the boundary provides an intrareservoir trap that pools hydrocarbons adjacent to the facies interface.

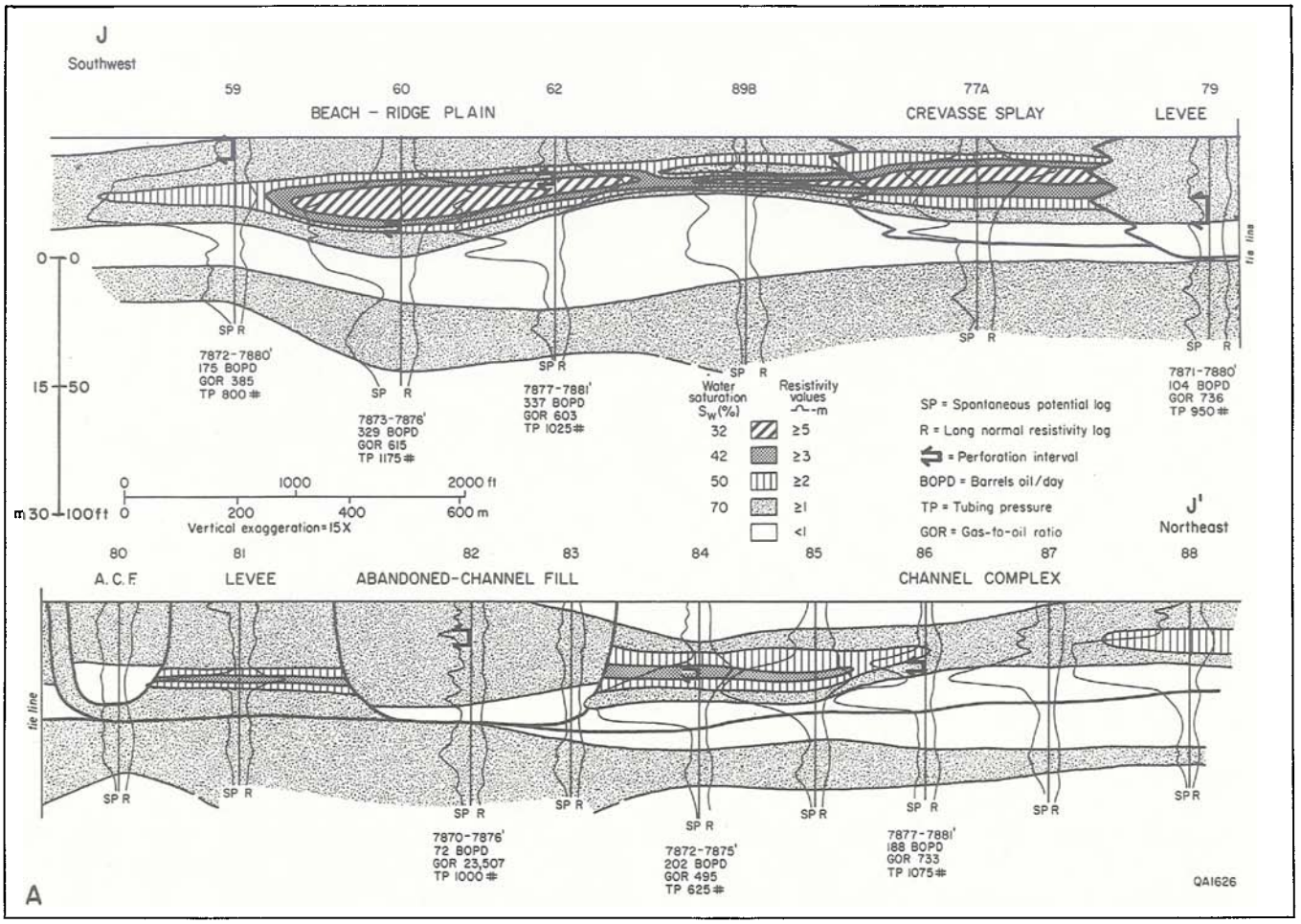

Figure 13. Resistivity cross sections, east Cayce reservoir: (A) section J-J' is drawn using the top of the Cayce sandstone as a datum, and (B) section I-I' is drawn on a structural datum. Contours of resistivity values facilitate the evaluation of the internal continuity of sandstone facies. Lines of sections shown in figure 8.

Reservoir Drainage Characteristics

Water-Influx Trends

Water-cut maps show the amount of water produced as a percentage of the total fluid production (oil, gas, and water) from each production well. The progressive influx of water into the Cayce reservoir for 40 years is shown in figure 15. Water influx in the east Cayce displays two distinct geometries. A broad zone of edge-water influx began in the northwest section by 1950 (fig. 15A). This swath of higher water cuts migrated progressively southward. However, channelized migration was the dominant mode of water influx in the eastern part of east Cayce reservoir (fig. 15A). With time, this dip-oriented water-invasion channel expanded laterally (fig. 15B) until 1970, when most of the east Cayce wells were producing more than 90 percent water. Watered-out and abandoned wells are also shown in figure 15; the pattern of abandonment of watered-out wells follows the same trends shown during early water invasion. In the west Cayce reservoir, channelized water influx dominated; minor edge-water invasion occurred on the west side of the field (fig. 15C).

Water-influx trends relate directly to the architecture of the reservoir sandstone. Zones of channelized invasion correspond well to the crosscutting, upward-fining fluvial-channel system

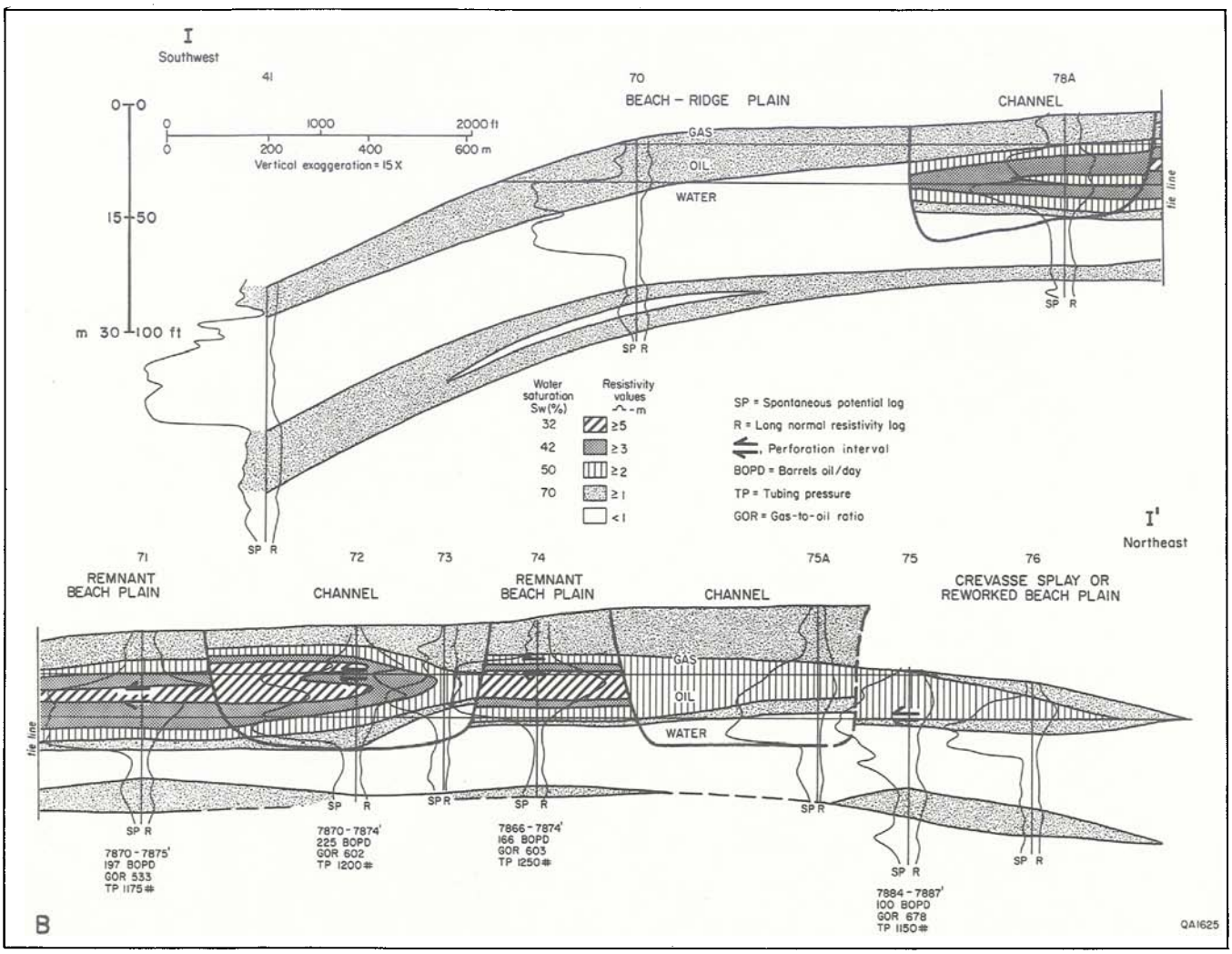

Figure 13. (continued)

in both reservoirs (fig. 15C). The broad zones of edge-water influx are within the laterally continuous and widespread beach-ridge plain sandstones of east Cayce and within the delta-front and shoreface sandstones of west Cayce. Certain facies retard water invasion, most notably the multiple delta-fringe sands of west Cayce, which are characterized by serrate SP patterns. This central zone of low water production may also be due to the structurally high position of the facies on the crest of the dome. Other facies displaying low water productions are levee and sand-poor abandoned-channel-fill and marsh deposits. In general, these argillaceous interbedded sand and mud facies are characterized by production with higher gas-to-oil ratios than those of the associated fluvial-channel and beach-ridge plain sandstones.

Reservoir Productivity

Average annual production from each well from the discovery of the reservoir (1942) to 1965 and from 1966 to 1982 was contoured on maps (fig. 16). Productivity trends are digitate in areal geometry and strongly dip oriented, particularly for the early production from east Cayce reservoir. There is a suggestion of similar production trends and orientations in the west Cayce; however, because

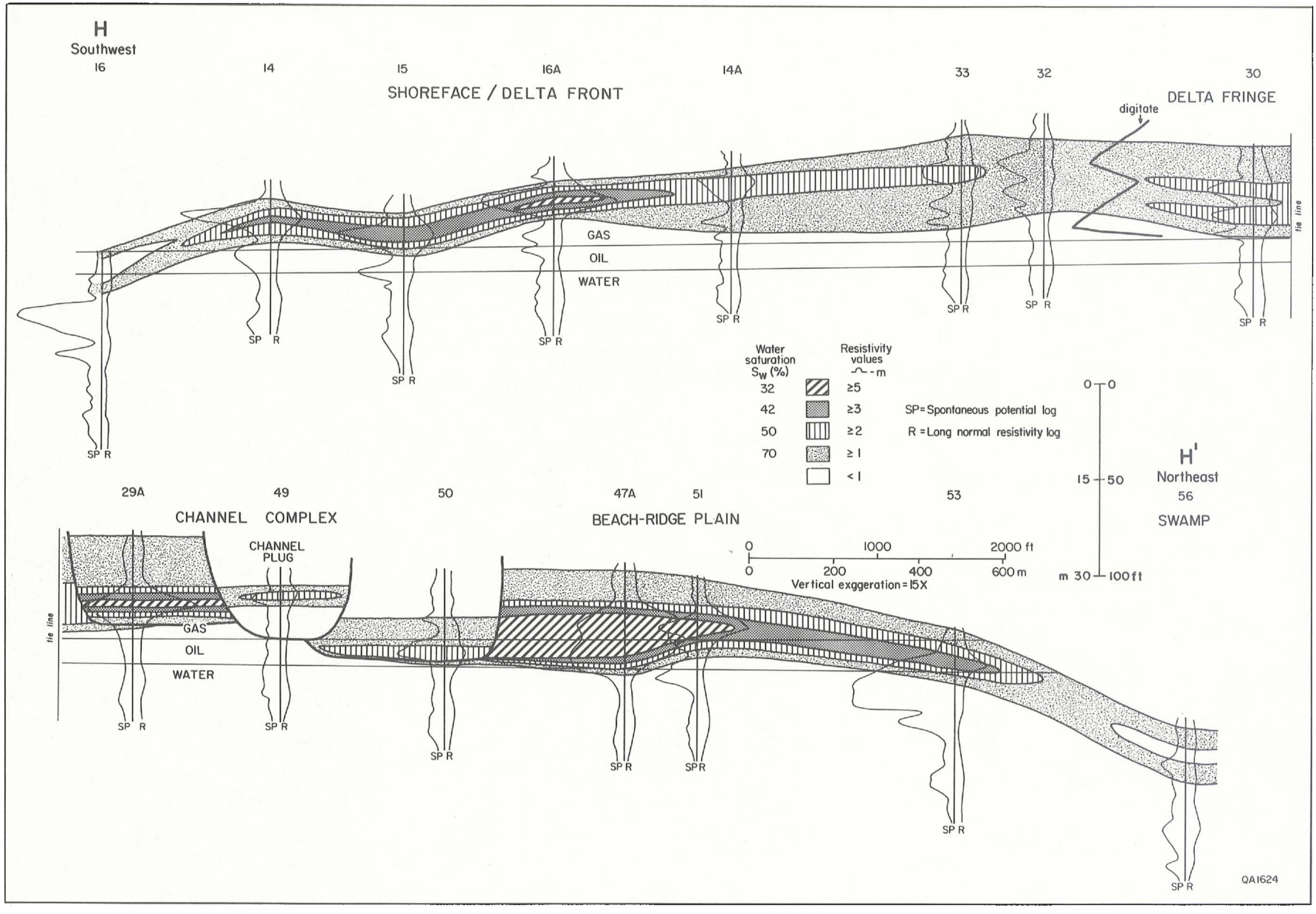

Figure 14. Resistivity cross section, west Cayce reservoir. Hydrocarbon distribution is most continuous in strandplain sandstones. Line of section shown in figure 8.

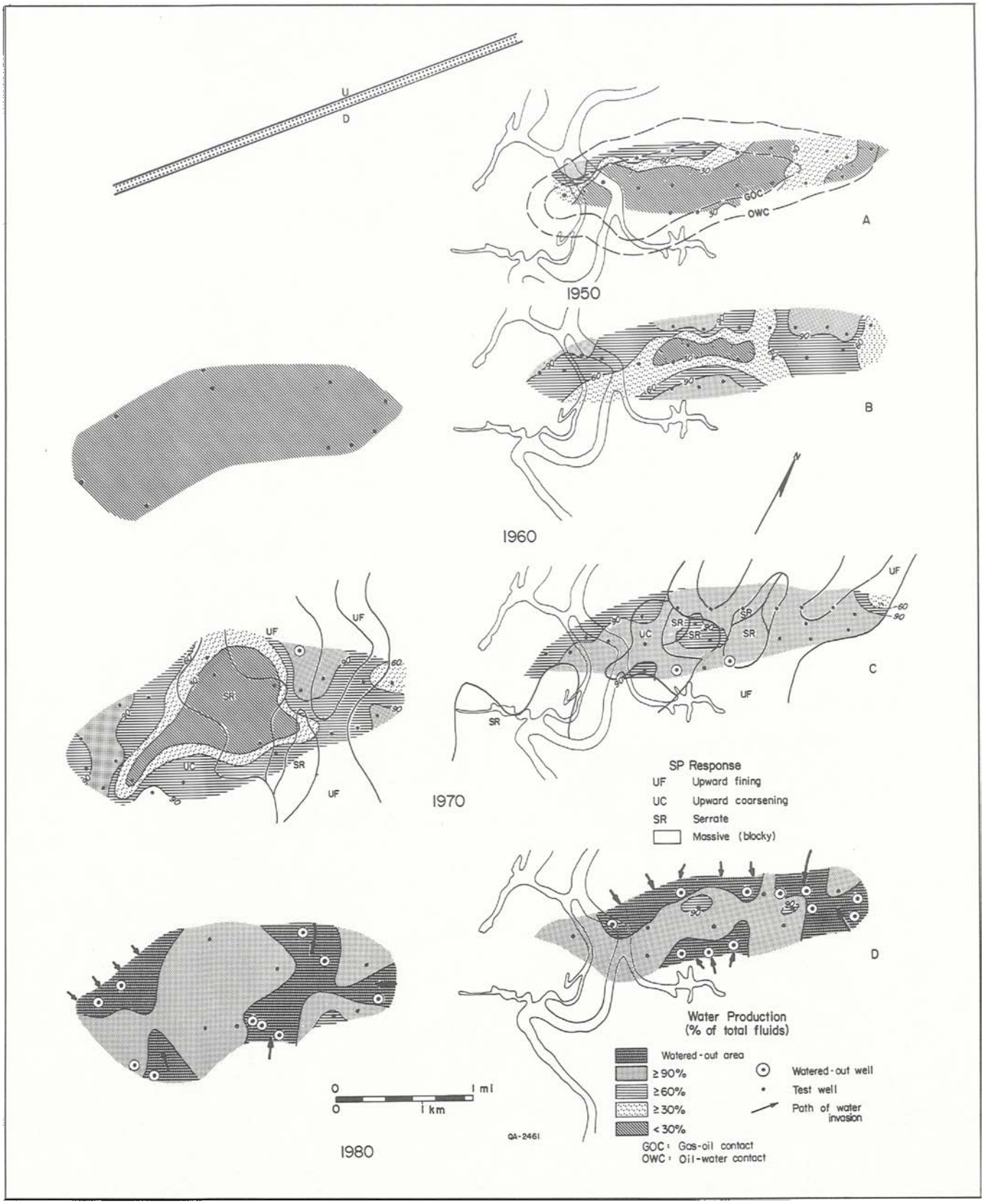

Figure 15. Sequential water-cut maps, east and west Cayce reservoirs. Crosscutting fluvial channel sandstones clearly focus water influx. In contrast, strandplain sandstones are characterized by broad fronts of water influx.

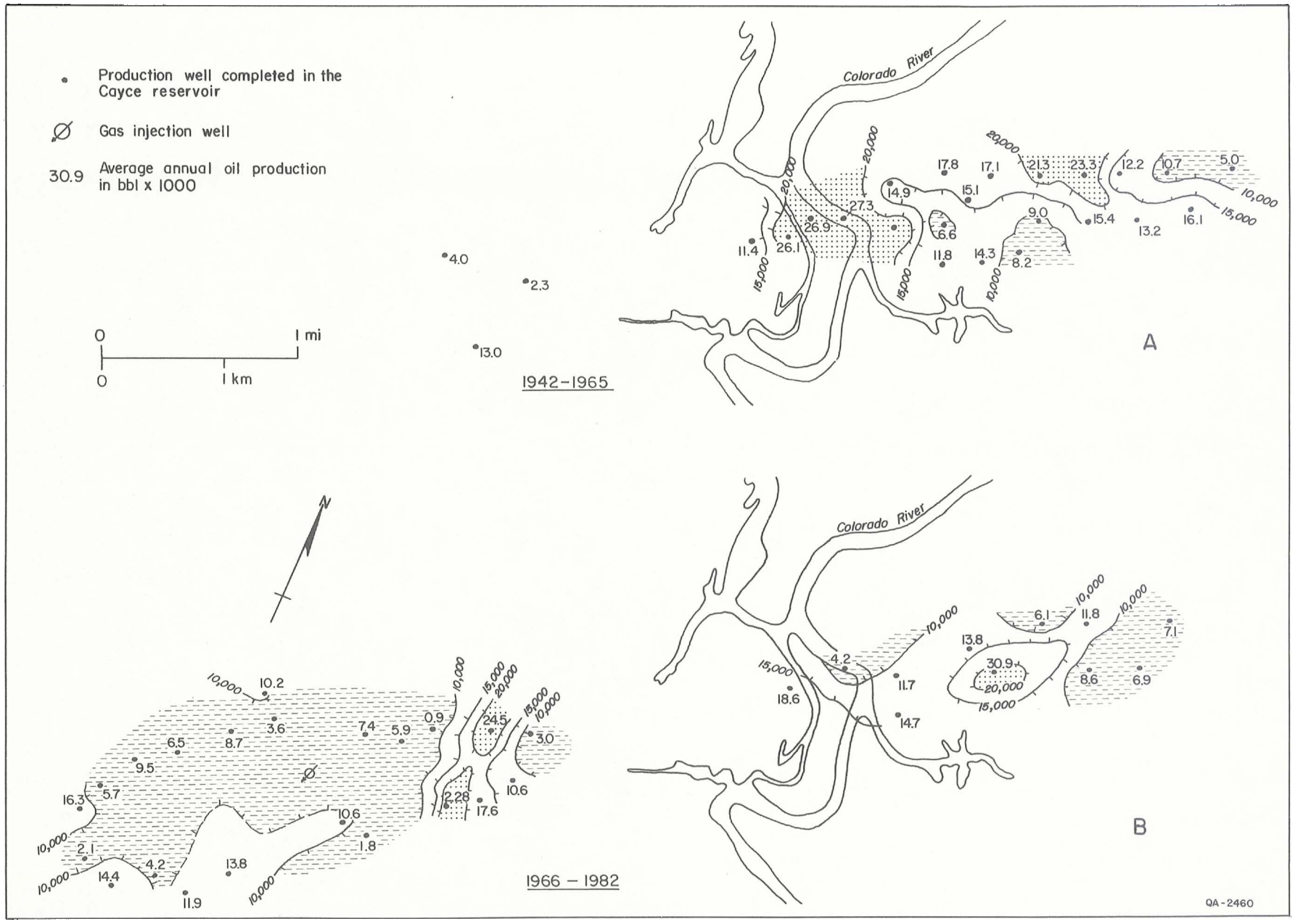

Figure 16. Reservoir productivity maps of (A) the east Cayce reservoir for the period 1942 through 1965 and (B) the east and west Cayce reservoirs for the period 1966 through 1982.

this reservoir produces from a thin oil rim, production patterns are poorly defined.

During the early years of production (1942 to 1965), the east Cayce yielded a little over 8.0 million barrels of oil. Much of the oil was derived from two major dip-oriented trends (fig. 16): The western trend produced from laterally continuous beach-ridge plain and crevasse splay deposits, whereas the north-central trend tapped fluvial and associated remnant shore-zone sandstones. The central low-yield area that separates the axes of high oil productivity consists of mud-rich swamp and abandoned channel-fill deposits and adjacent levee sandstones. Recent production trends (1966 to 1982) relate more closely to structure than to stratigraphy, the central high-production area being localized over the crest of the anticline (fig. 16) and decreasing toward the encircling oil-water contacts.

The channellike dip-oriented zone of high oil production on the east flank of west Cayce reservoir (fig. 16B) corresponds approximately to the thick zone of hydrocarbon saturation shown by the resistivity cross section (fig. 14). On the basis of resistivity distribution, the presence of an intra-reservoir trap was postulated. The hydrocarbon seal in the strandplain sandstones was provided by a crosscutting fluvial channel. However, two of the most prolific wells in west Cayce reservoir are in the channel sandstone (fig. 16B). Closer examination of wells 50 and 47A in figure 14 reveals that the base of channel sandstone lies below the gas-oil contact, whereas most of the hydrocarbons in the strandplain lie within the gas cap. The oil-saturated zone at the base of the strandplain sandstone probably lies within immature and bioturbated shoreface sediments that were deposited during initial strandplain progradation. Thus, oil production from the channel sandstone was from the coarsest grained and presumably better quality reservoir, whereas strandplain production was from poor-quality reservoir sandstones.

CORNELIUS RESERVOIR: A PROGRADED MUD-RICH STRANDPLAIN COMPLEX

The Cornelius sandstone is separated from the underlying Cayce by a 50-ft (15-m)-thick lower-shoreface-to-shelf mudstone in the North Markham–North Bay City field area. The mudstone pinches out updip where the Cayce and Cornelius sandstones merge into a single unit along the shore-zone axis (fig. 5). Reservoir continuity is high parallel to the depositional axis of the sandstone but low seaward.

Depositional Environment

Sandstone Distribution

The Cornelius genetic unit displays a systematic seaward decrease in sandstone content. Sandstone content (60 percent) is greatest north of the field area and adjacent to the updip fault and decreases uniformly basinward. Isopach contours exhibit a strongly strike-parallel orientation (fig. 17). Detailed isopach maps of individual genetic reservoir units, such as the third Cornelius sandstone (CO-3; fig. 18, inset), record the presence of well-developed alternating axes of high and low sandstone content, suggesting a ridge-and-swale paleotopography. Areas with thick sandstones display straight seaward margins (fig. 18), and at least one of the thicks is characterized by the bifurcating morphology typical of chenier ridges. The most seaward thick is discontinuous, being interrupted by areas of thinner sandstone development.

Areal Distribution of Component Facies

Component facies of the Cornelius sandstone display a strong strike-parallel orientation and an elongate geometry (fig. 19) similar to sandstone distribution patterns. Progradational facies inferred

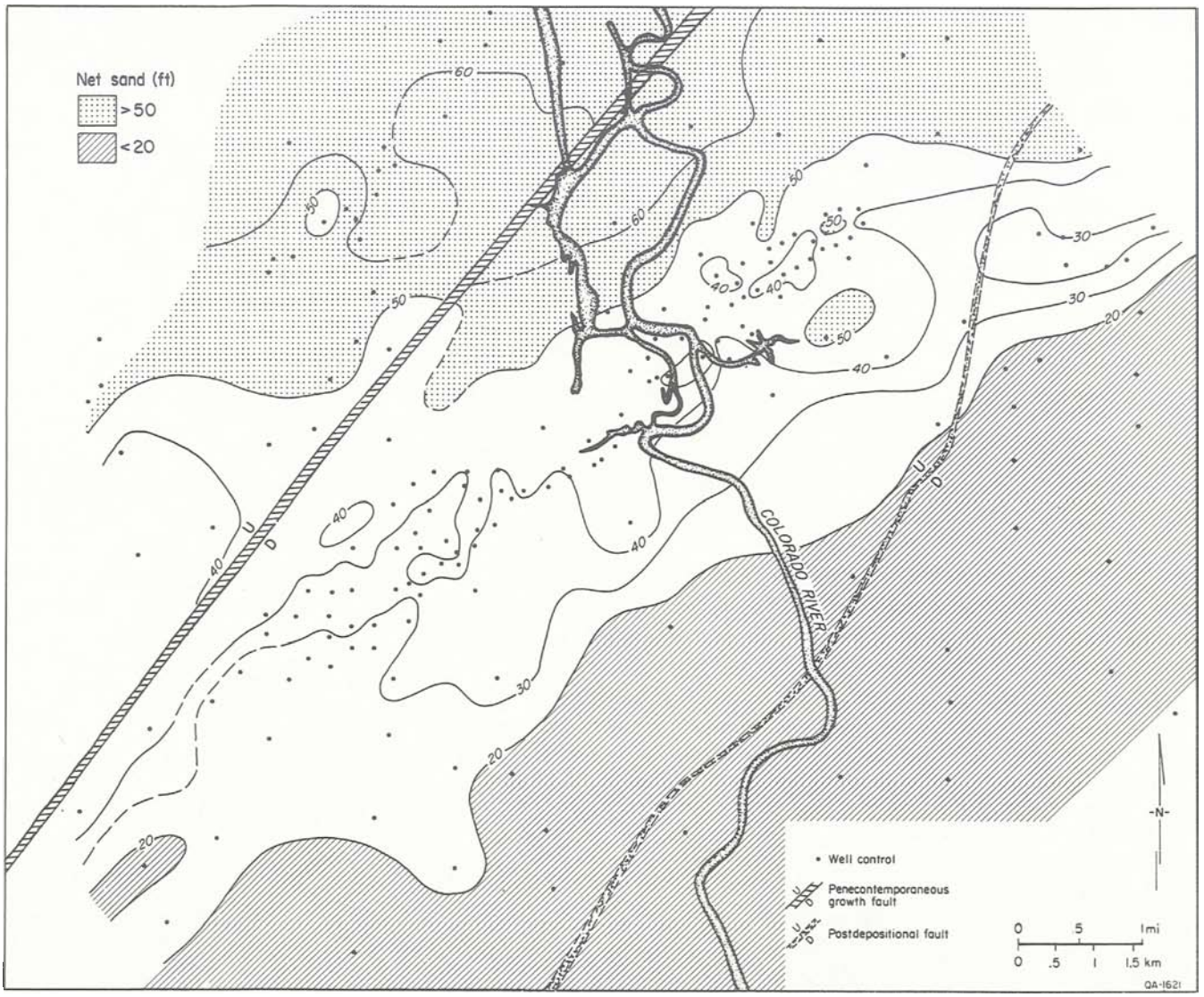

Figure 17. Net-sandstone map, Cornelius sandstone, showing a simple and systematic basinward decrease in sandstone content.

from upward-coarsening SP log motifs are concentrated landward, whereas aggradational and mixed SP facies characterized by upward-fining, serrate, and spiked patterns are more common seaward. This reversal of the typical arrangement of aggradational and progradational facies expected in a shore-zone system (contrast fig. 19 with fig. 10, for example) is further complicated by a broad zone of upward-fining deposits aligned parallel to the shoreline and located seaward of the principal progradational facies (fig. 19). Note that the log-character map shows the log facies anatomy of only the third Cornelius (CO-3) genetic unit (fig. 19, inset), which is the principal oil sand in the Cornelius, but does not show the log character of the entire Cornelius sandstone. The CO-3 genetic unit shales out near the downdip fault.

Interpretation of Depositional Environments

The strong strike-parallel orientation of component facies and the seaward decrease in sandstone content in the field area suggest that the Cornelius sandstone is the product of sedimentation on the seaward side of a prograding

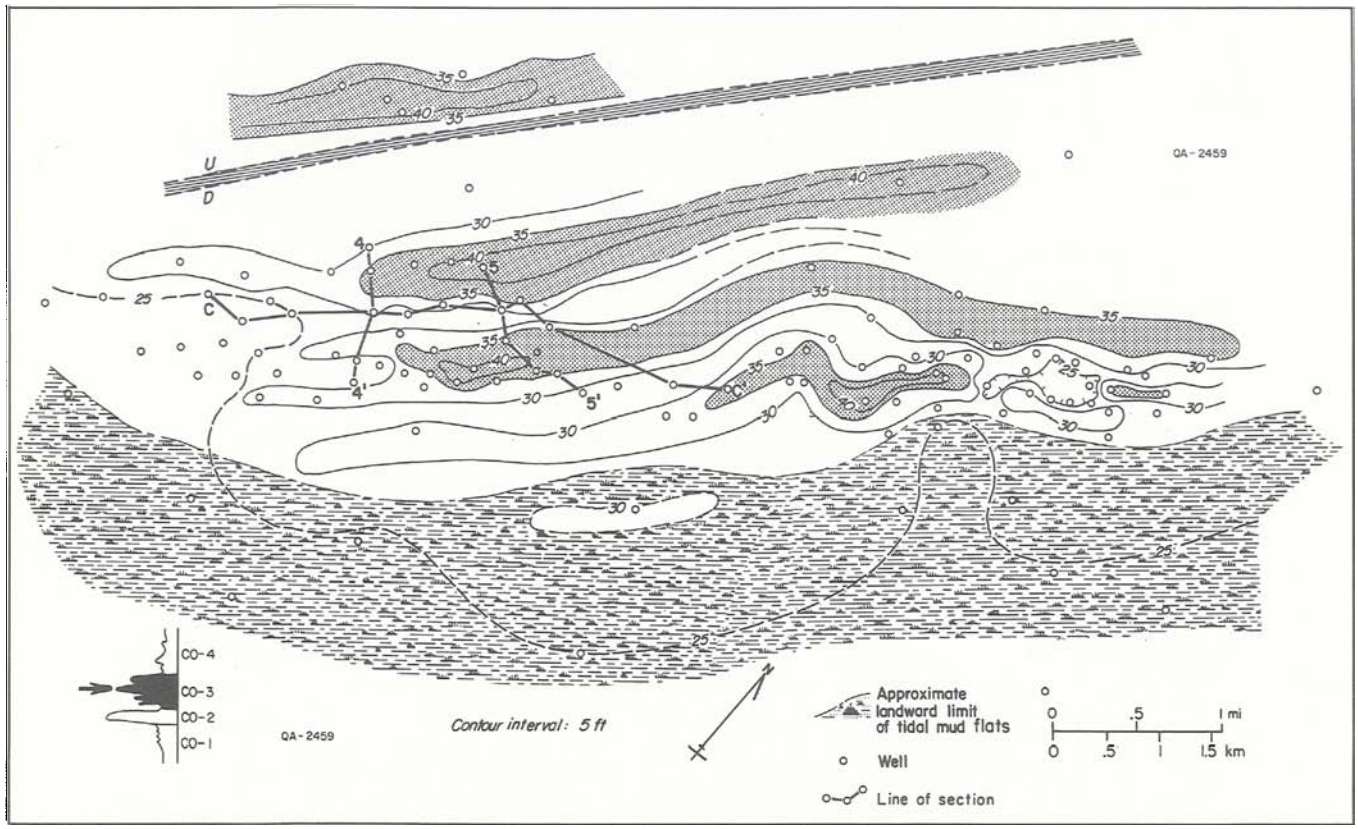

Figure 18. Detailed net-sandstone map of the third Cornelius sandstone (CO-3, see inset), illustrating an area of alternating sandstone thicks and thins that lie immediately landward of tidal mud-flat facies. Cross sections 4-4′ and 5-5′ are shown on figure 20 and cross section C-C′ is shown on figure 21.

shore-zone system. Reservoir-specific dip sections (fig. 20A) substantiate the progradational nature of the deposit. Further clues to the origin of the reservoir are the morphology of the sandstone thicks mapped in the CO-3 genetic unit (fig. 18) and the broad strike-parallel expanse of aggradational deposits (intertidal mud flats) immediately seaward of the progradational facies tract. The area of alternating sandstone thicks and thins represents a beach-ridge-and-swale complex. Bifurcating beach ridges are common along modern chenier plains, particularly near estuaries (fig. 3). SP log patterns of the ridge complex are dominantly progradational but also include upward-fining and blocky motifs, indicating that the processes responsible for their formation were diverse.

The zone of upward-fining sediments seaward of the beach-ridge complex was deposited in a subtidal to intertidal mud-flat system. Modern mud flats along the western Louisiana coastline exhibit similar textural trends ranging upward from the fine sand of the breaker-bar zone (inner shoreface) through very fine sand and sandy mud of the middle tidal flat to the mud, clay, and sandy mud of the upper tidal flat (Beall, 1968). Tidal mud flats originate by rapid sedimentation in a protected swale landward of a breaker-bar system. In the Cornelius reservoir, the breaker-bar deposits exhibit serrate or spiked SP motifs of sand encased in lower shoreface and mud-flat mudstone.

The paleomorphology of the Cornelius sandstone is similar to the physiography of modern chenier plains. Sandstone content in the Cornelius (20 to 50 percent in the field area), however, is much higher than the characteristically low (less than 20 percent) average sandstone content in Holocene chenier plain deposits. Furthermore, development of chenier plains requires an abundant supply of mud, such as that of the modern river-chenier couplets of the Mississippi, Amazon, and Orinoco Rivers. Mud-rich delta systems were absent during Frio deposition (Galloway and others, 1982).

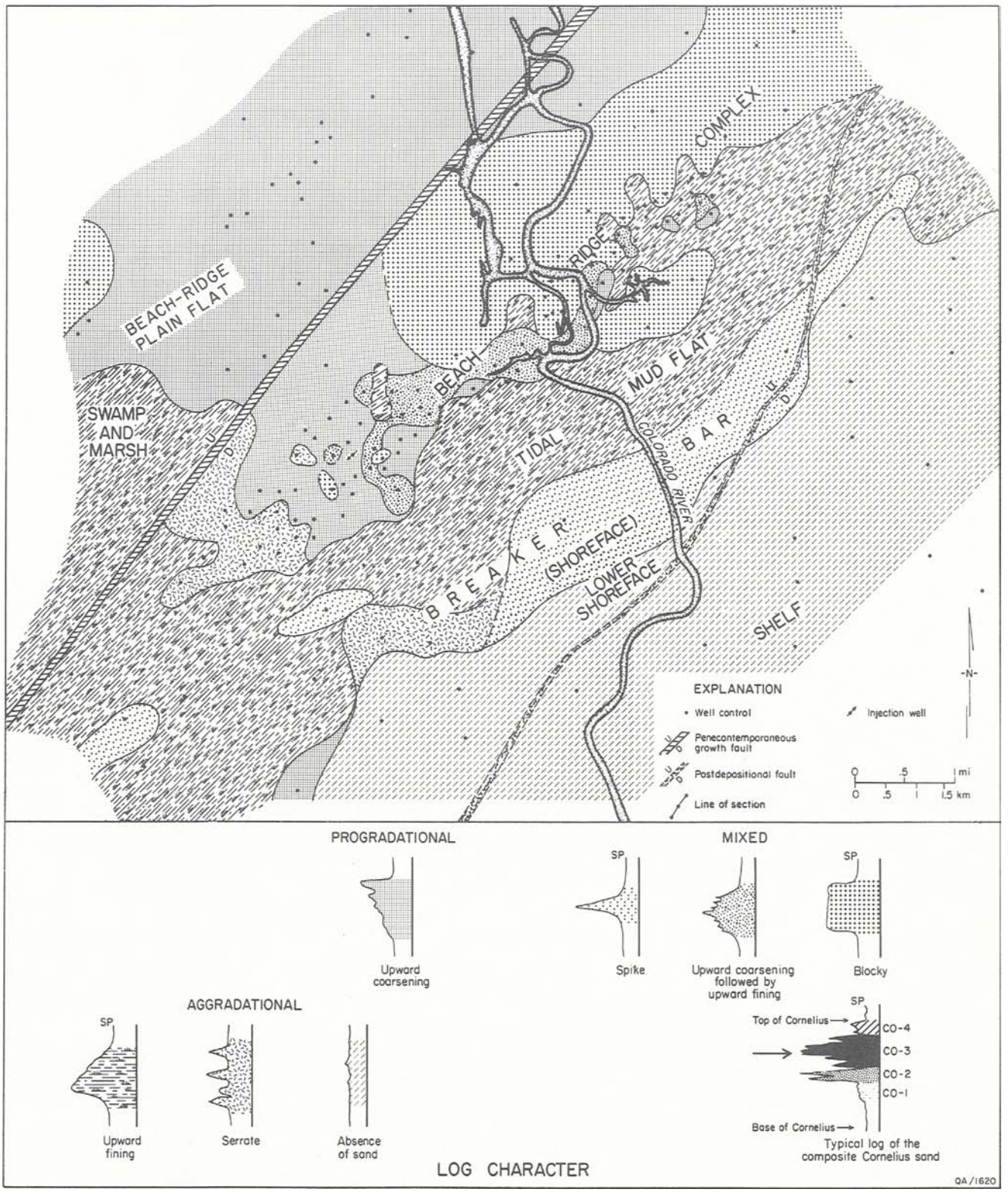

Figure 19. Interpretive facies anatomy of the third Cornelius (CO-3, see log) sandstone. The strike-parallel alignment of component facies matches net-sandstone trends and suggests shore-zone sedimentation. The beach-ridge complex is composed of the alternating ridges and swales mapped in figure 18. Thin breaker-bar and possibly beach deposits formed a shoal seaward of the complex, allowing deposition of fine-grained sandstone and mudstone under sheltered conditions in the intervening area. The tidal mud-flat facies rest on sandstones and siltstones of the shoreface and therefore exhibit an upward-fining textural trend.

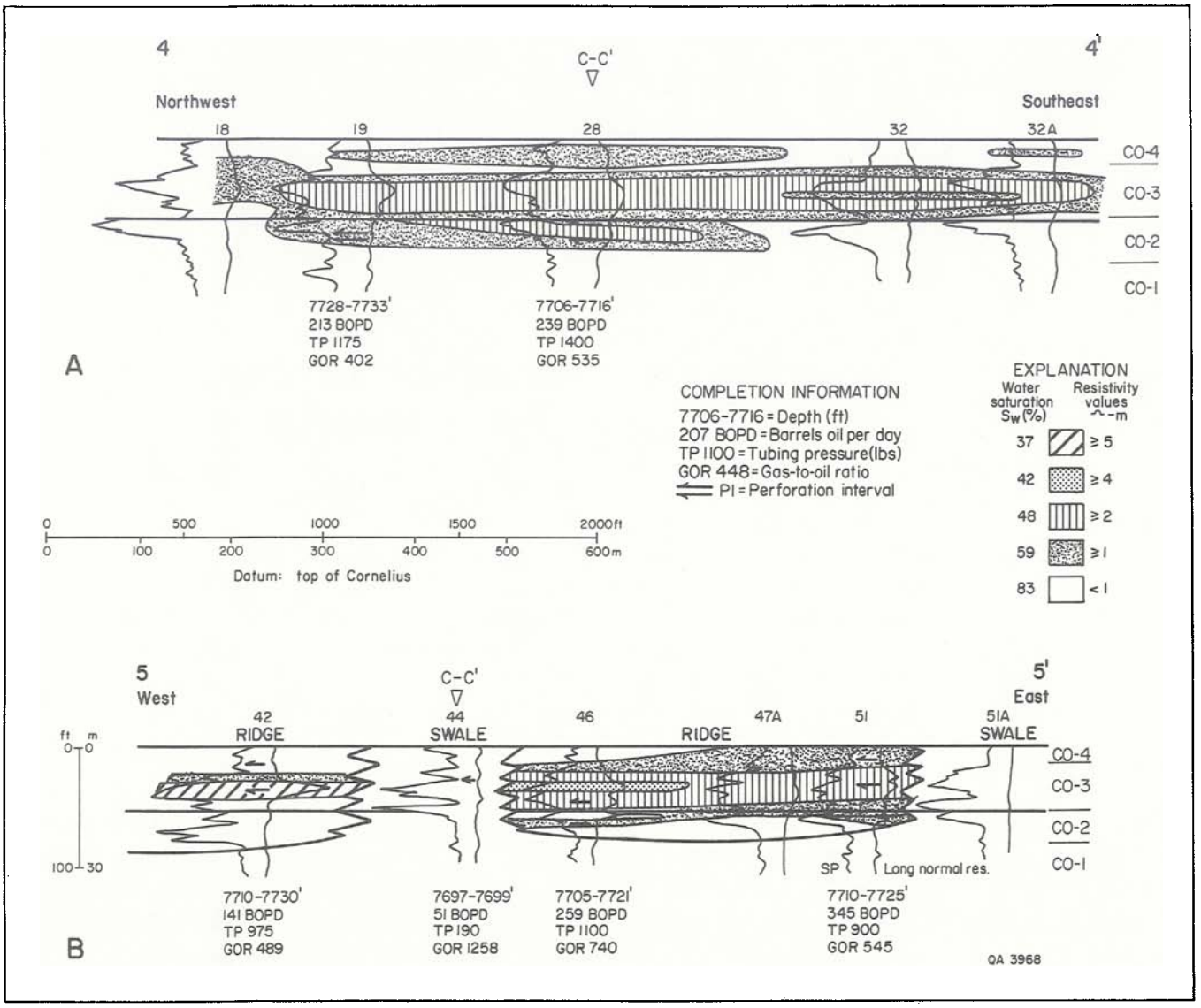

Figure 20. Resistivity dip sections, Cornelius sandstone, showing (A) the relatively continuous zones of hydrocarbon saturation in marginal deposits and the offlapping relation of the second and third Cornelius sandstones (CO-2 and CO-3). Hydrocarbons in the lower sandstone are trapped against the bounding surface separating the two sandstone units. (B) Section through the beach-ridge plain core emphasizing the localization of hydrocarbons in the ridge facies and the restriction of interridge continuity by intervening swales. Lines of sections shown in figure 18.

Therefore, the complex Cornelius beach-ridge plain is probably intermediate, in both composition and process, between mudstone-rich chenier plain deposits and sandstone-rich beach-ridge plain systems. Consequently, the Cornelius is interpreted to have been deposited in a mudstone-rich beach-ridge plain system.

Landward of the beach-ridge complex lies a broad expanse of progradational deposits designated "beach-ridge plain flat" on figure 19. SP logs typically exhibit simple or serrate upward-coarsening trends. The origin of this sandstone-rich area is enigmatic, requiring examination of whole cores (which, unfortunately, are not available) to conclusively interpret depositional subenvironments. Paleoenvironments that may be represented are washover fans on the marshy coastal plain and bay and bay-fill deposits.

Reservoir Continuity and Hydrocarbon Distribution

The continuity of mudstone-rich beach-ridge plain reservoirs varies highly. Beach-ridge facies exhibit great lateral continuity parallel to the shore zone. Normal to the shore zone, however, continuity is variable to poor. Cross sections showing resistivity values (figs. 20 and 21) illustrate the impersistent and nonuniform distribution of hydrocarbons in ridge and interridge areas. Where strong ridge-and-swale paleotopography exists, the continuity between chenier and adjacent upward-fining interridge deposits is poor (figs. 20B and 21, wells 27 to 58). Initial potential tests of wells perforated in ridge sandstones displayed high initial productions and pressures (averages of 230 barrels of oil per day and 1,175 psi, respectively, fig. 20) and low gas-to-oil production ratios, whereas wells in the muddier swale deposits were characterized by high gas-to-oil production ratios and low initial yields and pressures, regardless of location on the structure. Thus, mudstone-rich beach-ridge plain reservoirs can be characterized as composite bodies composed of a series of stringerlike subreservoirs that may or may not be isolated from adjacent bodies by intervening swales. Interbedded sandstones of washover origin in the swales contain hydrocarbons and furthermore may act as conduits between subreservoirs.

The well-defined thick and thin sandstone trends of the ridge-and-swale facies grade marginally into broad areas of similar sandstone content, indicating a widespread tidal sand flat on the flanks of the beach-ridge complex (fig. 18, southwest quadrant). Here, hydrocarbon distribution (figs. 20A and 21) is uniform in the reservoir.

A second class of subreservoir is present in the Cornelius. The Cornelius reservoir is composed of four genetic units (CO-1 to CO-4). The upper two units, and in particular the CO-3 sandstone, contain most of the oil and gas; however, hydrocarbons are also trapped in the lower units. A dip cross section illustrates the relation between the upper and lower hydrocarbon subreservoirs (fig. 20A). The upper zone of hydrocarbon saturation lies in beach plain sandstones (CO-3) that have prograded across more distal and slightly older deposits (CO-2). The updip part of the CO-2 sandstone appears to have been partly reworked into the younger cycle so that the older cycle pinches out against the base of the CO-3 sandstone. Resistivity trends follow this pattern and indicate two stacked zones of hydrocarbon saturation. On the basis of completion data, we conclude that the sandstone units are interconnected, as tubing pressures are fairly similar regardless of completion level. However, the average initial oil yield from the upper sandstone was 25 percent higher than that from the lower sandstone.

Reservoir Drainage Characteristics

Water-Influx Trends

As in the Cayce reservoir, the depositional fabric of the Cornelius strongly influenced reservoir drainage patterns, particularly during the first 30 years of production. Sequential water production maps illustrate ridges of high water cut separated by troughs of lower water production (fig. 22, 1950, 1960). The strike-parallel linear zones of high water influx conform to the axes of the beach ridges in the CO-3 sand, and troughs separating high water-cut zones correspond to interridge swales. The production (hydrologic) gradient between producing wells can be extremely steep. In adjacent wells (only 660 ft, 200 m, apart) in the northeast quadrant of the west Cornelius reservoir, production was 28 percent water from one and 95 percent water from the other (fig. 22, 1960). Similar steep gradients characterize the northwest and southeast margins of the reservoir during all three time intervals that were mapped.

The northeast and, to a lesser extent, southwest quadrants were the principal zones of water influx into the reservoir. The seaward (southeast) flank was characterized by low water influx throughout early production because that area of the reservoir lies adjacent to the landward pinch-out of the tidal mud flats (fig. 19). These mud-rich deposits functioned as an aquiclude, restricting updip migration of water to the beach-ridge facies. In contrast, water influx into the reservoir from the northeast and southwest expanded laterally so that by 1970 most of the wells in the crest of the reservoir were producing more than 90 percent water. By 1980 all the wells displayed water production greater than 90 percent, and much of the reservoir

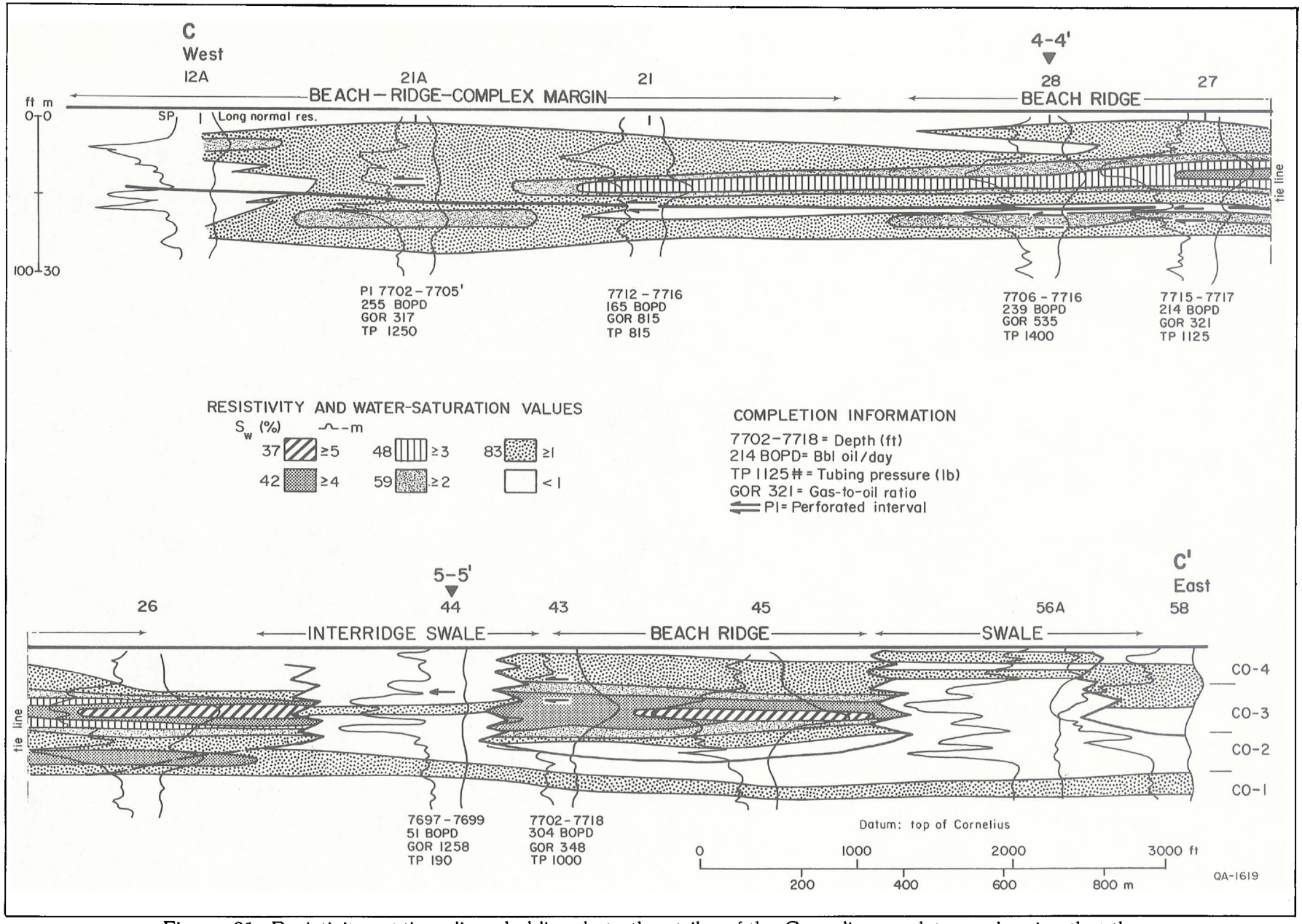

Figure 21. Resistivity section aligned obliquely to the strike of the Cornelius sandstone, showing that the zone of hydrocarbon impregnation in beach-ridge sandstones is interrupted by the intervening swales. Line of section shown in figure 18.

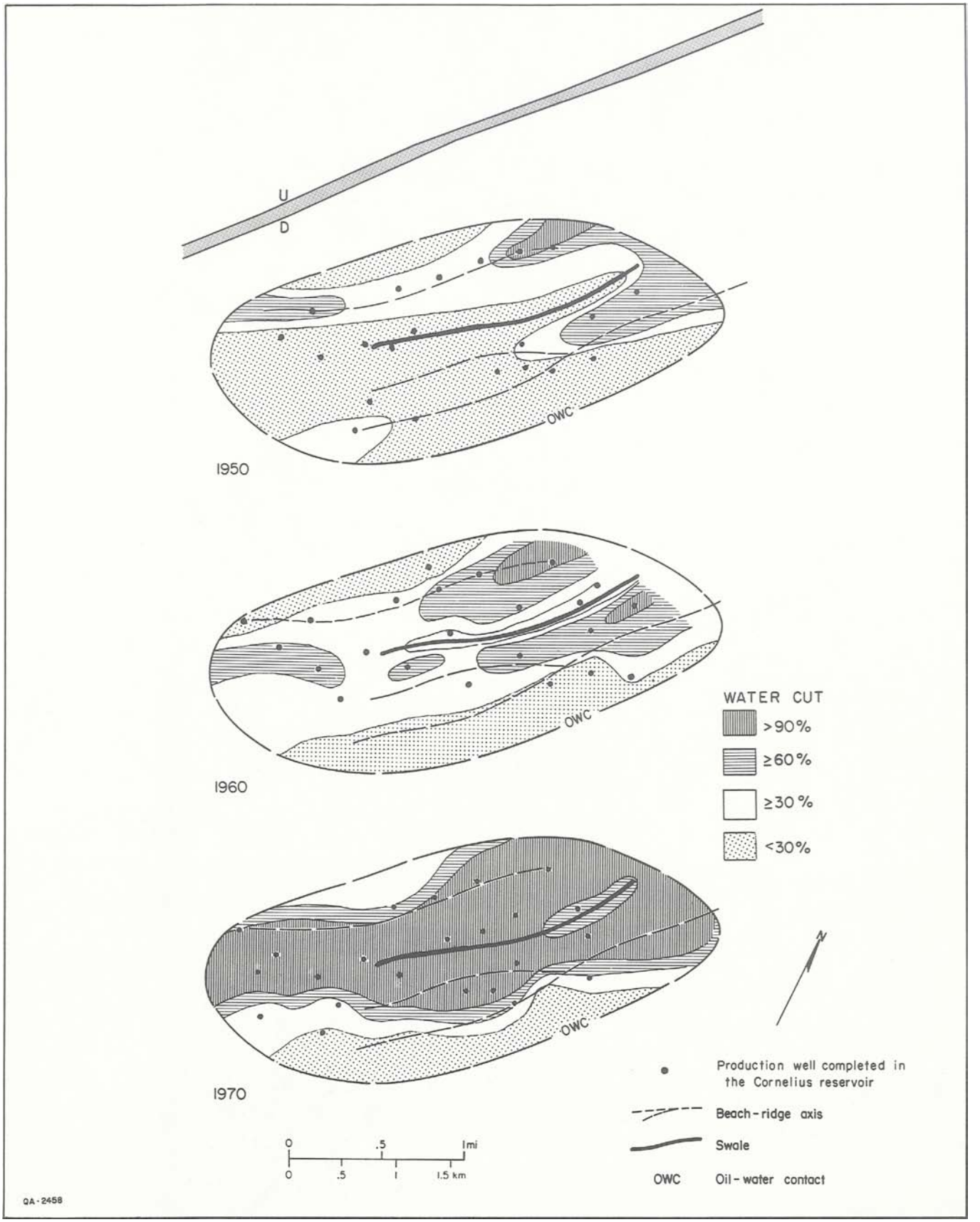

Figure 22. Sequential water-cut maps of the west Cornelius reservoir. Ridge facies focus water influx. The tidal mud-flat deposits south of the reservoir restricted water invasion from that direction.

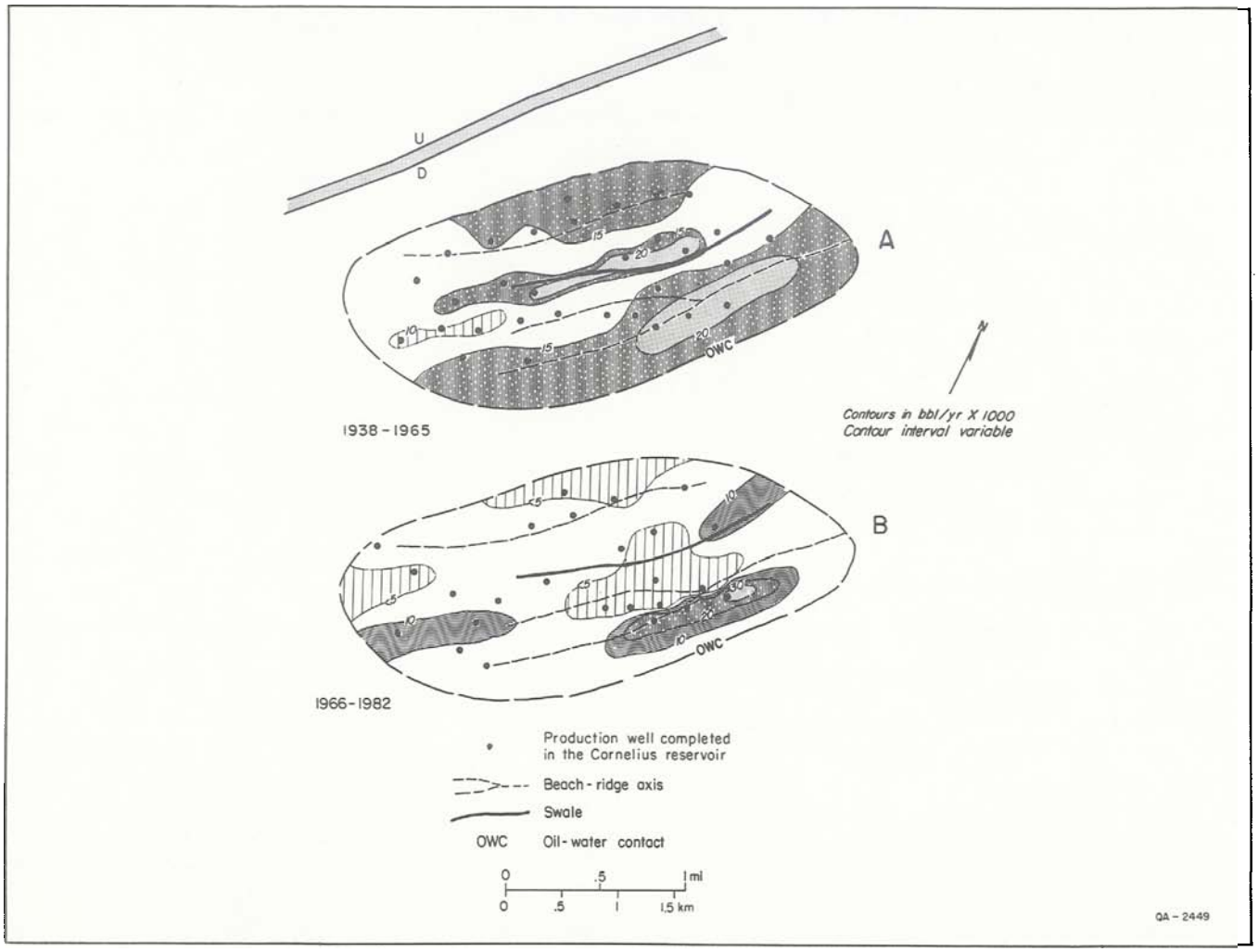

Figure 23. Reservoir production maps, west Cornelius reservoir, (A) 1938 through 1965 and (B) 1966 through 1982. Production trends coincide with the facies arrangement of the Cornelius.

had watered out, abandoned areas corresponding closely to the areas of high initial water cut.

Reservoir Productivity

Oil production trends in the west Cornelius conform to the facies architecture of the reservoir. Contoured well-by-well yields are linear and match sandstone distribution patterns. In general, the more productive wells produce from beach-ridge facies and the less productive wells from interridge areas (fig. 23). However, this is by no means a definitive rule. Substantial early production was from interridge deposits located over the crest of the anticline. Wells producing from this linear tract averaged more than 20,000 barrels of oil per year during the first 26 years of production. Subsequent production from this area however was relatively poor, averaging less than 5,000 barrels per year from 1966 to 1982 (fig. 23B). In contrast, wells perforated in beach-ridge sandstones continuously produced higher amounts of oil relative to the remaining reservoir area. For example, wells in the southeast quadrant of west Cornelius produced more than 20,000 barrels of oil per year from 1938 to the end of 1982. As a broad generalization, wells completed in swale deposits are more rapidly depleted and display higher gas-to-oil ratios and lower initial yields and pressures than do wells draining beach-ridge sandstones.

CARLSON RESERVOIR: A TRANSGRESSED BEACH-RIDGE PLAIN

The Carlson sandstone represents the penultimate phase of major sandstone deposition in the upper Frio Formation (fig. 5). It is overlain by lower shoreface and shelf mudstones that seal the reservoir and that are in turn overlain by the Greta barrier sandstone. Spontaneous potential curves of the Carlson reservoir typically suggest an initial progradational phase followed by aggradation during coastal onlap.

Depositional Environment

Sandstone Distribution

Sandstone distribution in the Carlson interval exhibits a well-defined strike-parallel elongation similar to that of the Cornelius sandstone. The area of maximum sand accumulation (90 ft, 27 m, or 50 percent of the Carlson unit) lies adjacent to (both updip and downdip of) the major growth fault in the field area. Sandstone content systematically decreases southeastward from the fault. As in the Cayce reservoir, sandstone contents decrease over the crest of the rollover anticline.

Areal Distribution of Component Facies

Analysis of SP logs of the Carlson sandstone generally shows a lower, thick, upward-coarsening sandstone overlain by a thinner, upward-fining sandstone (fig. 5, well 48). However, at least five variations of this mixed progradational-aggradational cycle exist (fig. 24). Simple aggradational facies are present but are only locally developed. Note that the log-facies map of the Carlson reflects the genetic character of the entire sandstone package rather than that of individual genetic units.

The Carlson sandstone contains three principal facies (fig. 24). In the southern and southeastern parts of the field area, upward-coarsening progradational facies are prevalent, but much of the rest of the area is characterized by a basal serrate upward-coarsening sandstone, overlain by a blocky sandstone, which is in turn overlain by an upward-fining cycle (SP log motif PA-3, fig. 24). At the boundary between the areal occurrences of these two major facies components is a third sandstone having the basal progradational cycle capped by a well-defined blocky sandstone (log motif PA-2, fig. 24). The latter log motif, PA-2, has a well-defined strike-parallel geometry; along strike, sandstones adjacent to it display simple or serrate upward-fining upper zones. Other log facies of lesser abundance are narrow, dip-oriented aggradational facies and localized progradational facies over the crest of the rollover anticline.

Interpretation of Depositional Environments

The Carlson reservoir is a composite sandstone deposited within a prograding strandplain system that was partly reworked during subsequent transgression. The lower progradational phase is a simple but widespread unit of upward-coarsening sandstones, in contrast to the more complex facies relation of the overlying transgressive deposits. Sandstones that exhibit blocky SP responses are probably of wave-modified deltaic origin, as suggested by the lobate geometry and strike parallelism of the facies. Fluvial feeder systems are the aggradational deposits updip of the deltaic sandstones and another channel system characterized by dip-oriented blocky sandstones to the southwest (fig. 24).

The upward-fining SP log patterns that cap much of the Carlson sandstone reflect the superposition of lower-shoreface and shelf mudstones over coarser shore-zone clastics during transgression. In modern transgressive shore-zone settings such as that of Matagorda Peninsula, Texas, coastal onlap is accompanied by shoreline erosion and washover-sheet and -fan deposition (Wilkinson and Basse, 1978). These processes cause the landward migration of the barrier or

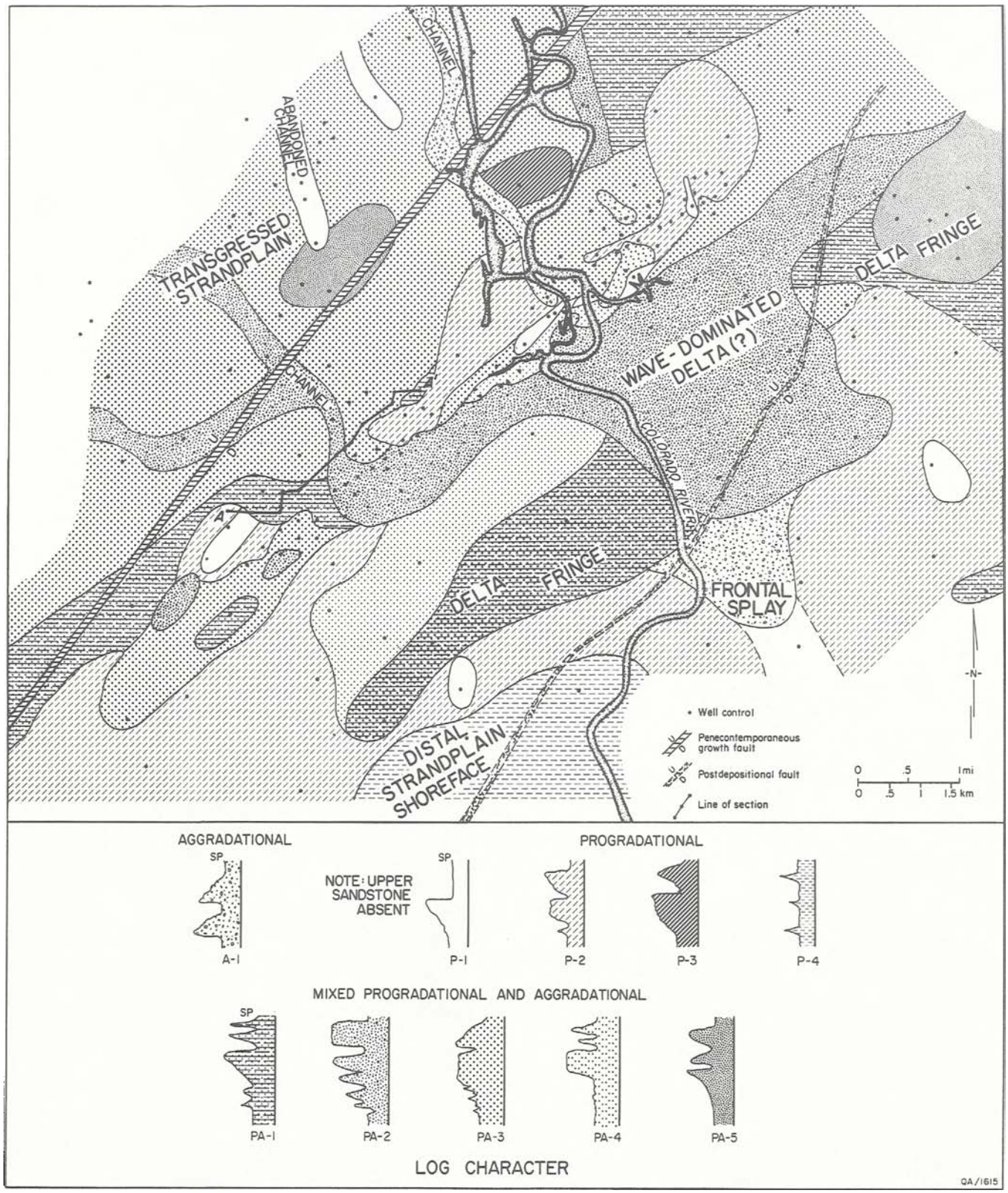

Figure 24. Log-facies map of the Carlson sandstone, illustrating the complex facies architecture of this composite strandplain deposit. Log-facies patterns commonly exhibit upward-coarsening (progradational) overlain by upward-fining (aggradational) trends. Purely progradational patterns downdip reflect shoreface or delta-front sedimentation or both. Section A-A′ shown in figure 25.

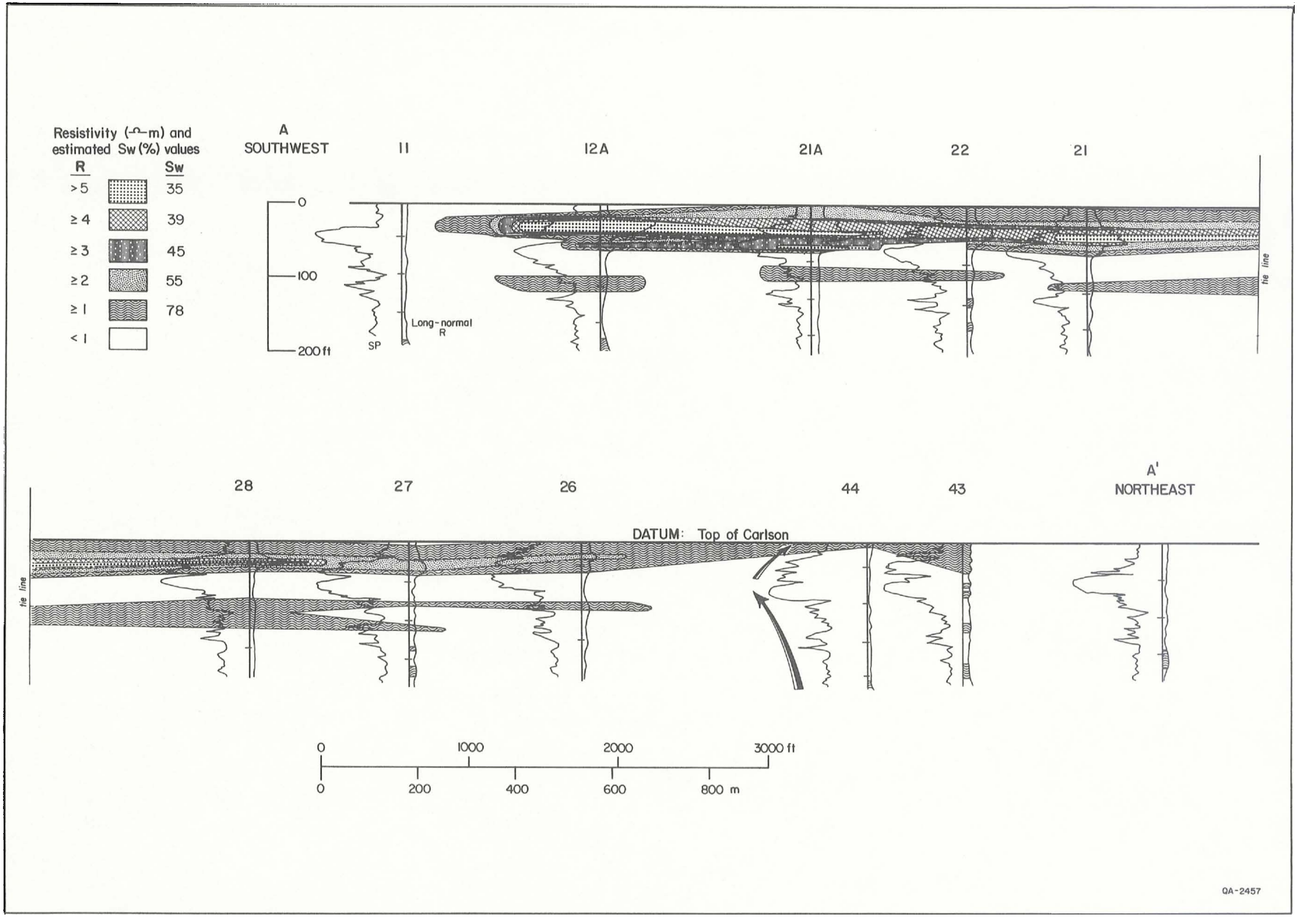

Figure 25. Resistivity cross section, Carlson reservoir, emphasizing the lateral continuity of the hydrocarbon-bearing transgressed strandplain sandstones. Line of section shown in figure 24.

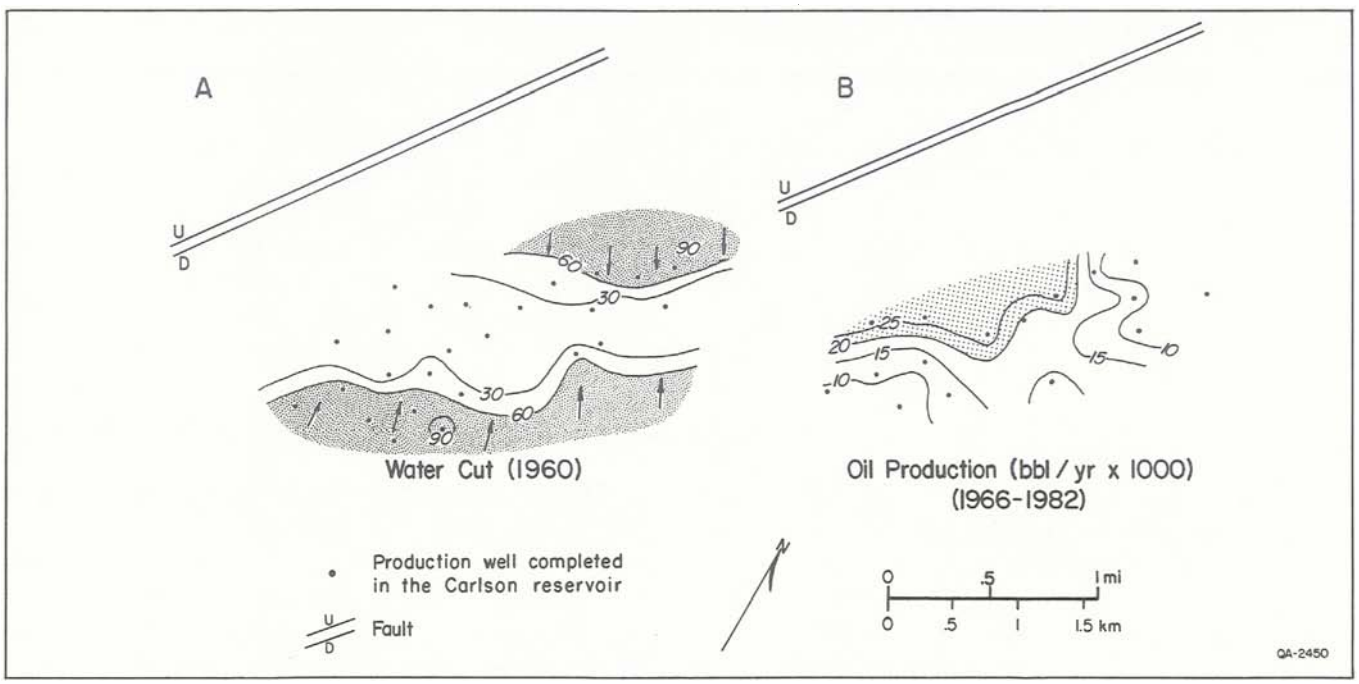

Figure 26. Water-cut (A) and production (B) maps of the Carlson reservoir.

strandplain (Morton and McGowen, 1980). The resultant transgressive sand bodies exhibit a tabular geometry. However, transgression may be episodic and not necessarily continuous. During temporary stillstands in the Carlson transgression, wave-dominated deltas were deposited (fig. 24). Similar episodic transgressive events accompanied by periodic delta progradation have been recognized in Holocene sediments below Matagorda Peninsula (Wilkinson and Basse, 1978).

Reservoir Continuity

Although the facies architecture of the Carlson sandstone is complex, the distribution of hydrocarbons within the reservoir is continuous along both strike and dip (fig. 25). Most of the hydrocarbon column lies within sheetlike transgressive deposits. Although the distribution of hydrocarbons is uninfluenced by facies changes, the thickness and vertical continuity of the hydrocarbon-bearing zone depends greatly on the facies. The thickest and most vertically homogeneous hydrocarbon impregnations occur in massive or simple upward-fining sandstones; the hydrocarbon-saturated zone in wells characterized by serrate upward-fining sandstones is thinner and heterogeneous. The overall pattern of hydrocarbon occurrence is one of uniform lateral continuity and variable vertical continuity within the transgressed strandplain sandstones.

Reservoir Drainage Trends

Water influx into the Carlson reservoir takes place along broad edge-water fronts rather than by areally restricted or channellike invasion. Early water incursion took place in two wide zones on the updip and downdip edges of the field (fig. 26A) and gradually expanded toward the crest of the reservoir. Watered-out and abandoned areas correspond well to the areas of early edge-water encroachment. Hydrocarbon production patterns are simple (fig. 26B), a further indication that the facies anatomy of the Carlson sandstone exerted little influence on production trends. The simple patterns of water influx and the uniform production trends confirm the conclusion that the reworked Carlson strandplain sandstones have uniform lateral continuity and that facies changes in this setting do not impart strong lateral heterogeneity to the sandstone body.

CONCLUSIONS

The oil-productive strandplain sandstones of the North Markham–North Bay City field yield reservoir continuity models for three microtidal strandplain systems. Each reservoir type displays characteristic water-influx and oil production patterns. These trends (and variations) can be attributed to the facies architecture of the reservoir.

Reservoir Models

The composite and progradational beach-ridge plain/wave-dominated delta sandstone (fig. 27) of the Cayce reservoir is clearly heterogeneous. Macroscopic heterogeneities in this sandstone prevent, hinder, or enhance intrareservoir fluid flow. Dip-oriented sandstones of distributary-channel origin focus early water influx into the reservoir. These sandstones also influence the distribution of hydrocarbons by sealing local compartments of the reservoir, creating intrareservoir traps, thereby restricting hydrocarbon migration in the adjacent strandplain deposits. The boundaries between juxtaposed facies may be characterized by lithologic changes (channel sandstone/floodplain mudstone) where mudstone is an aquitard or by sandstone-on-sandstone contacts (channel sandstone/beach-ridge deposits). Flow-resistant facies boundaries result from the contrasting physical and textural characters of the adjacent facies. Divergent grain-size distributions, pore-space distributions, internal stratification, frequency and position of shale breaks, permeability distributions, and directional permeability all hinder fluid movement between facies and contribute to different production characteristics. In addition to flow resistance caused by internal physical and textural differences, thin mud coatings such as those on lateral accretion surfaces may impede flow across facies boundaries. Detailed subsurface analysis of the Holocene Rio Grande delta clearly shows that channel sands are separated from adjacent sand facies (channel and floodplain) by a thin mud sheath (fig. 17 in Fulton, 1975) that hinders fluid migration between facies. Although reasons for the flow-resistive function of facies boundaries have not been clarified in the literature, an increasing number of papers are describing anomalous drainage patterns in composite sandstone bodies having complex facies interrelationships.

In the sandstones of beach-ridge plain origin that comprise the bulk of the Cayce reservoir (fig. 27), fluid influx takes place along broad fronts, possibly only locally and partly hindered by beach-face accretion surfaces. Permeability increases upward, and heterogeneity is least parallel to the long axis of the ridges.

Productive sandstones in mudstone-rich beach-ridge plain reservoirs such as the Cornelius are elongate parallel to the paleoshoreline and are separated by mudstone-rich interridge swales (fig. 28). Initial production is strongly influenced by paleophysiography. Elongate beach ridges focus water influx. During late-stage primary production, the influence of the ridge facies on the water cut diminishes, and the entire reservoir becomes characterized by high water production. Wells completed in beach-ridge sandstones display continuously higher oil production rates relative to the remaining reservoir area; by contrast, wells perforated in sandstones deposited in interridge areas (storm-washover deposits, and so forth), which also may display high initial productions, exhibit a more rapid decline in production.

Reservoir continuity is greatest in the marine transgressive deposits (fig. 29) of the North Markham–North Bay City field. The hydrocarbons in the Carlson reservoir are contained within a transgressive sandstone that rests on an underlying progradational strandplain sequence. The distribution of the oil and gas pool is uninterrupted by facies changes, and the water-influx and production characteristics of the reservoir appear to be uninfluenced by the facies architecture of the sandstone. The tabular geometry of the transgressive sandstone results in similar production characteristics from broad areas of the reservoir.

Oil Recovery and Fluid Injection

Recovery efficiencies of the entire spectrum of sand-rich and intermediate composition strandplain

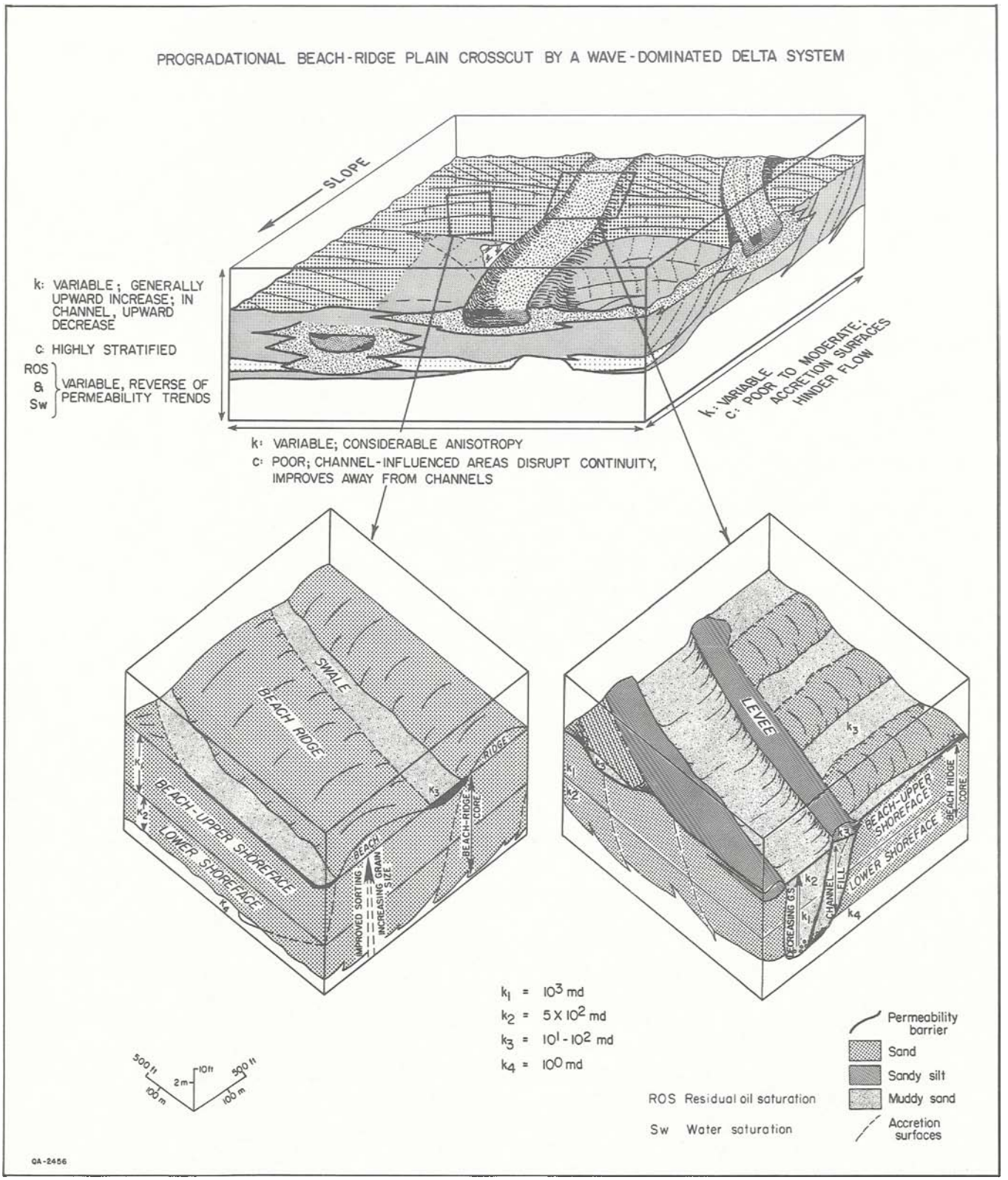

Figure 27. Continuity of a composite progradational beach-ridge strandplain transected by a fluvial-deltaic system modeled on the Cayce reservoir. Reservoir continuity decreases with increasing complexity of the crosscutting system such that macroscopic heterogeneity is greatest at the interfaces between the fluvial, deltaic, and strandplain systems. Reservoir quality improves upward in strandplain and deltaic sandstones, but basal units of fluvial sandstones are the most porous and permeable.

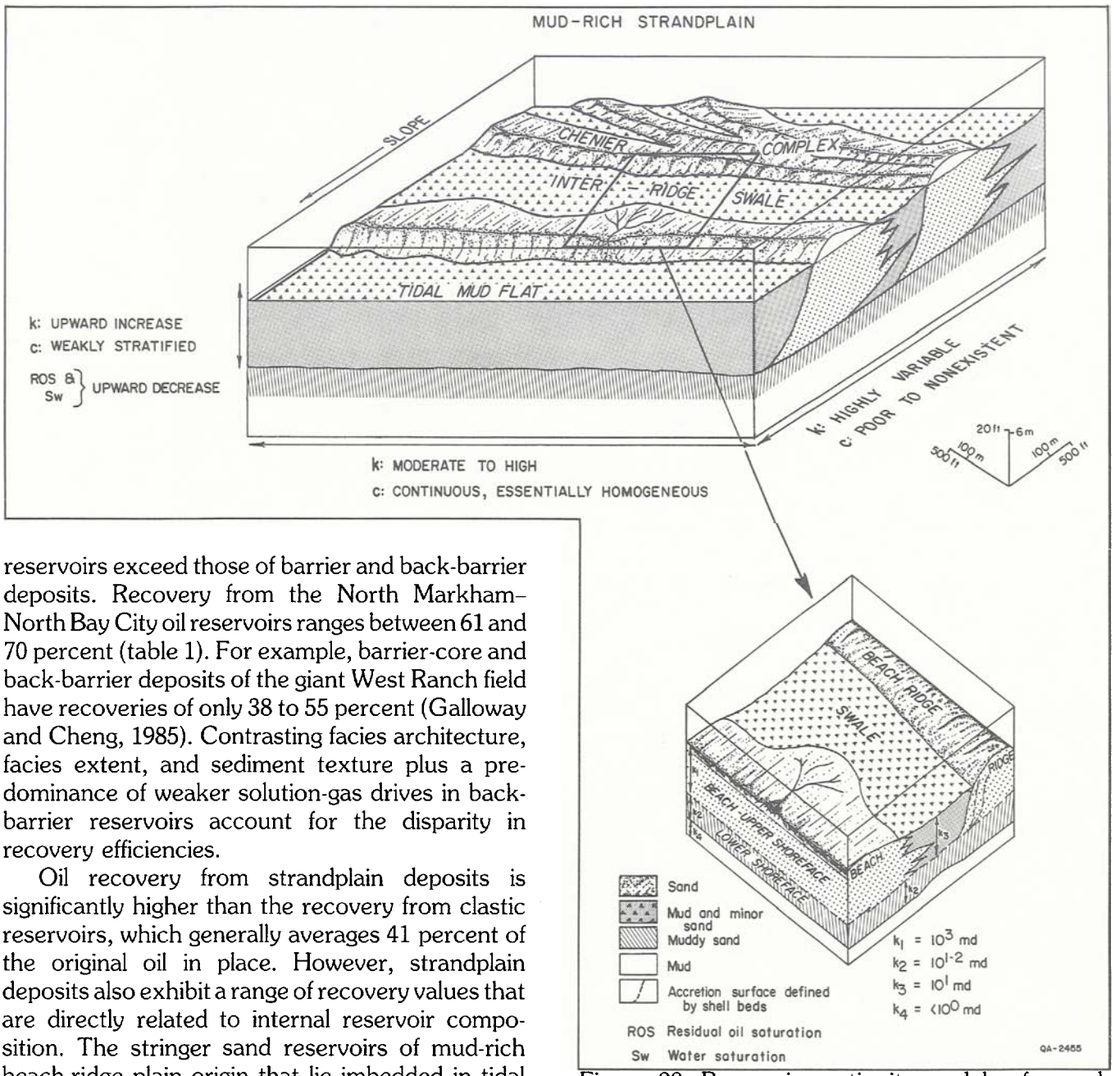

Figure 28. Reservoir continuity models of a mud-rich beach-ridge plain complex based on data from the Cornelius sandstone. These reservoirs display great continuity parallel to the depositional axis but poor to nonexistent continuity between adjacent ridges.

reservoirs exceed those of barrier and back-barrier deposits. Recovery from the North Markham–North Bay City oil reservoirs ranges between 61 and 70 percent (table 1). For example, barrier-core and back-barrier deposits of the giant West Ranch field have recoveries of only 38 to 55 percent (Galloway and Cheng, 1985). Contrasting facies architecture, facies extent, and sediment texture plus a predominance of weaker solution-gas drives in back-barrier reservoirs account for the disparity in recovery efficiencies.

Oil recovery from strandplain deposits is significantly higher than the recovery from clastic reservoirs, which generally averages 41 percent of the original oil in place. However, strandplain deposits also exhibit a range of recovery values that are directly related to internal reservoir composition. The stringer sand reservoirs of mud-rich beach-ridge plain origin that lie imbedded in tidal mud-flat deposits exhibit lower recoveries (61 percent of the original oil in place) than the sand-rich, but highly heterogeneous, composite beach-ridge plain/deltaic complex (66 percent of the original oil in place). The most efficient oil recovery is from tabular transgressive deposits, where 70 percent of the original oil in place is being recovered by primary and secondary methods.

Anisotropic fluid migration patterns in strandplain reservoirs directly result from the complex facies architecture of these deposits. Injected fluids would most likely display migration patterns similar to those exhibited by the autochthonous reservoir fluids. Thus, mapping of the extent and distribution of facies and of the primary fluid migration patterns is essential to the success of secondary and tertiary recovery projects.

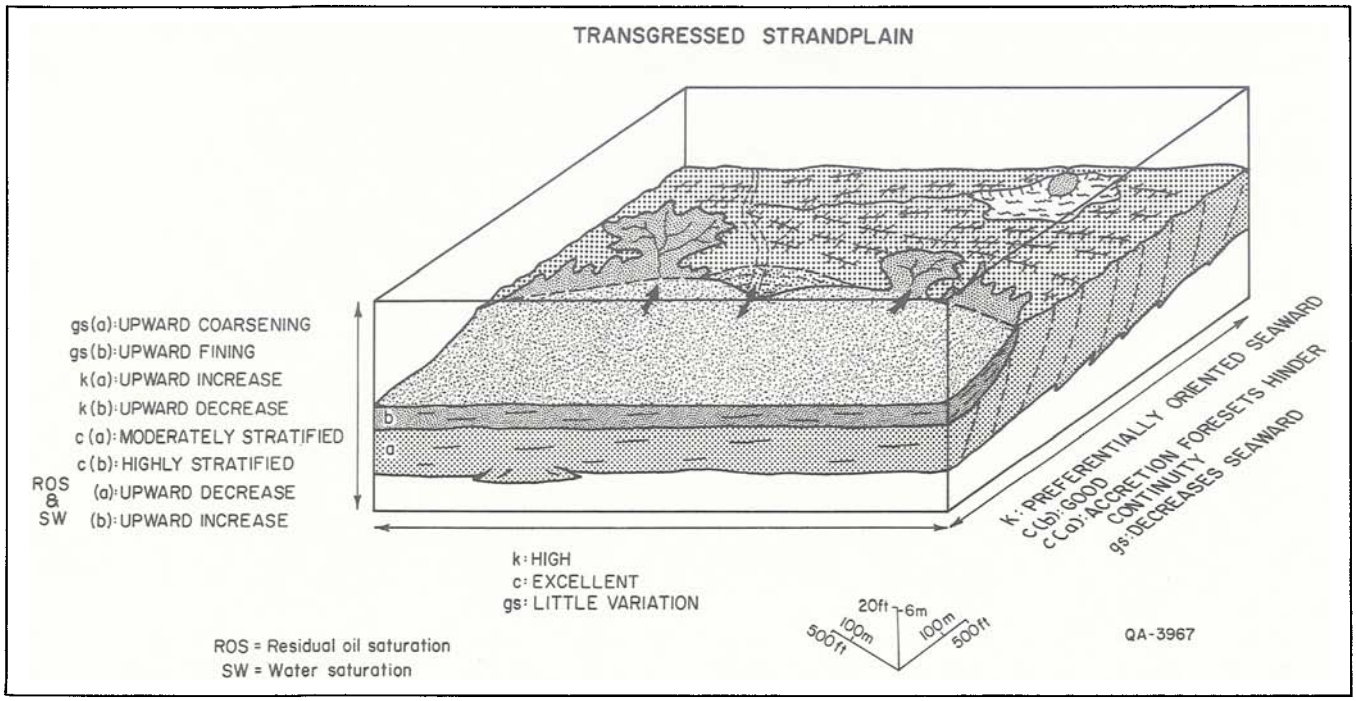

Figure 29. Reservoir continuity model of transgressed strandplain sandstones based on data from the Carlson sandstone. Although the facies architecture of the reservoir is complex, the physical and textural characteristics of juxtaposed facies are similar, facilitating continuous hydrocarbon distributions and broad fronts of water incursion as in simple progradational strandplain deposits.

ACKNOWLEDGMENTS

This study was funded by the U.S. Department of Energy, Division of Geothermal Energy, under contract no. DE-AC08-79ET27111, and by the Texas Energy and Natural Resources Advisory Council, Energy Development Fund, project no. 82-O-U-1. Marathon Oil Co., Shreveport, Louisiana, supplied production data from the North Markham–North Bay City field.

This manuscript benefited from reviews by L. F. Brown, Jr., J. R. DuBar, R. J. Finley, W. L. Fisher, W. E. Galloway, Z. S. Lin, R. A. Morton, and S. J. Tewalt.

Word processing was by M. J. Franklin and Shelley G. Gilmore, under the supervision of Lucille C. Harrell. The figures were drafted by John T. Ames, Mark T. Bentley, Jana Brod, Margaret Koenig, and Jamie McClelland, under the supervision of R. L. Dillon, and text illustration camerawork was by J. A. Morgan. The cover and text were designed by Jamie S. Haynes, and the manuscript was edited by R. Marie Jones-Littleton.

REFERENCES

Alpay, O. A., 1972, A practical approach to defining reservoir heterogeneity: Journal of Petroleum Technology, v. 24, p. 841-848.

Asquith, G. B., and Gibson, C., 1982, Basic well log analysis for geologists: American Association of Petroleum Geologists, Methods in Exploration Series, 216 p.

Beall, A. O., 1968, Sedimentary processes operative along the western Louisiana shoreline: Journal of Sedimentary Petrology, v. 38, no. 3, p. 869-877.

Brower, A., 1953, Rhythmic depositional features of the East Surinam coastal plain: Geologie en Mijnbouw, v. 15, p. 226-236.

Curray, J. R., Emmel, F. J., and Crampton, P. J. S., 1969, Holocene history of a strandplain, lagoonal coast, Nayarit, Mexico, *in* Castañares, A. A., and Phleger, F. B., eds., Coastal lagoons: a symposium: Universidad Nacional Autonoma de Mexico, p. 63-100.

Fisk, H. N., 1955, Sand facies of recent Mississippi delta deposits: Proceedings, Fourth World Petroleum Congress, sec. 1/C, p. 377-398.

Fulton, K. J., 1975, Subsurface stratigraphy, depositional environments, and aspects of reservoir continuity—Rio Grande delta, Texas: University of Cincinnati, Ph.D. dissertation, 314 p.

Galloway, W. E., and Cheng, E. S., 1985, Reservoir facies architecture in a microtidal barrier system—Frio Formation, Texas Gulf Coast: The University of Texas at Austin, Bureau of Economic Geology Report of Investigations No. 144, 36 p.

Galloway, W. E., Ewing, T. E., Garrett, C. M., Tyler, N., and Bebout, D. G., 1983, Atlas of major Texas oil reservoirs: The University of Texas at Austin, Bureau of Economic Geology Special Publication, 139 p.

Galloway, W. E., Hobday, D. K., and Magara, K., 1982, Frio Formation of the Texas Gulf Coast Basin—depositional systems, structural framework, and hydrocarbon origin, migration, distribution, and exploration potential: The University of Texas at Austin, Bureau of Economic Geology Report of Investigations No. 122, 78 p.

Gould, H. R., and McFarlan, E., Jr., 1959, Geologic history of the chenier plain, southwest Louisiana: Gulf Coast Association of Geological Societies Transactions, v. 9, p. 261-270.

Hartman, J. A., and Paynter, D. D., 1979, Drainage anomalies in Gulf Coast Tertiary sandstones: Journal of Petroleum Technology, v. 31, p. 1313-1322.

McCubbin, D. G., 1982, Barrier-island and strandplain facies, *in* Scholle, P. A., and Spearing, D., eds., Sandstone depositional environments: American Association of Petroleum Geologists Memoir 31, 410 p.

Morton, R. A., and McGowen, J. H., 1980, Modern depositional environments of the Texas coast: The University of Texas at Austin, Bureau of Economic Geology Guidebook 20, 167 p.

Otvos, E. G., and Price, W. A., 1979, Problems of chenier genesis and terminology—an overview: Marine Geology, v. 31, p. 251-263.

Polasek, T. L., and Hutchinson, C. A., Jr., 1967, Characterization of nonuniformities within a sandstone reservoir from a fluid mechanics standpoint: Proceedings, Seventh World Petroleum Congress, v. 2, p. 397-407.

Pryor, W. A., 1973, Permeability-porosity patterns and variations in some Holocene sand bodies: American Association of Petroleum Geologists Bulletin, v. 57, no. 1, p. 162-189.

Psuty, N. P., 1967, The geomorphology of beach ridges in Tabasco, Mexico: Louisiana State University, Coastal Studies Series No. 18, 51 p.

Railroad Commission of Texas, 1983, Annual report of the Oil and Gas Division for 1982: Austin, 733 p.

Tyler, Noel, Galloway, W. E., Garrett, C. M., Jr., and Ewing, T. E., 1984, Oil accumulation, production characteristics, and targets for additional recovery in major oil reservoirs of Texas: The University of Texas at Austin, Bureau of Economic Geology Geological Circular 84-2, 31 p.

Wells, J. T., and Coleman, J. M., 1981a, Periodic mudflat progradation, northeastern coast of South America: a hypothesis: Journal of Sedimentary Petrology, v. 51, no. 4, p. 1069-1075.

Wells, J. T., and Coleman, J. M., 1981b, Physical processes and fine-grained sediment dynamics, coast of Surinam, South America: Journal of Sedimentary Petrology, v. 51, no. 4, p. 1053-1068.

Wilkinson, B. H., and Basse, R. A., 1978, Late Holocene history of the central Texas coast from Galveston Island to Pass Cavallo: Geological Society of American Bulletin, v. 89, no. 10, p. 1592-1600.

Winker, C. D., 1979, Late Pleistocene fluvial-deltaic deposition, Texas Coastal Plain and shelf: The University of Texas at Austin, Master's thesis, 187 p.